A Medium-Resolution Near-Infrared Spectral Library of Late Type Stars: I.

Valentin D. Ivanov
European Southern Observatory, Karl-Schwarzschild-Str. 2, D-85748 Garching bei München, Germany
vivanov@eso.org

Marcia J. Rieke, Charles W. Engelbracht, Almudena Alonso-Herrero[1], George H. Rieke
Steward Observatory, The University of Arizona, Tucson, AZ85721, U.S.A.
mrieke, chad, grieke, aalonso@as.arizona.edu

Kevin L. Luhman
Harvard-Smithsonian Center for Astrophysics, 60 Garden Street, Cambridge, MA 02138, U.S.A.
kluhman@cfa.harvard.edu

ABSTRACT

We present an empirical infrared spectral library of medium resolution (R≈2000-3000) H (1.6 μm) and K (2.2 μm) band spectra of 218 red stars, spanning a range of [Fe/H] from ~-2.2 to $\sim+0.3$. The sample includes Galactic disk stars, bulge stars from Baade's window, and red giants from Galactic globular clusters. We report the values of 19 indices covering 12 spectral features measured from the spectra in the library. Finally, we derive calibrations to estimate the effective temperature, and diagnostic relationships to determine the luminosity classes of individual stars from near-infrared spectra.

This paper is part of a larger effort aimed at building a near-IR spectral library to be incorporated in population synthesis models, as well as, at testing synthetic stellar spectra.

Subject headings: atlases — infrared:stars — stars:abundances — stars:chromospheres — stars:fundamental parameters — stars:late-type

1. Introduction

Over the last two decades, evolutionary synthesis modeling has become a common tool to study unresolved stellar populations of galaxies in the optical and UV passbands (Bruzual & Charlot 1993; Worthey 1994; Vazdekis 1999; Leitherer et al. 1999). The heavy obscuration in starburst galaxies – often with $A_V \geq 5$ mag (Engelbracht 1997) – requires an expansion of these models into the near infrared (IR) domain, because the extinction there is reduced tenfold in comparison with the optical region: $A_K/A_V=0.112$ (Rieke & Lebofsky 1985). Therefore, it is not surprising that many studies of embedded stellar populations in galaxies have been conducted in the near-IR (Rieke et al. 1980, 1993).

IR evolutionary synthesis models based on synthetic spectra (Origlia, Moorwood & Oliva 1993; Kurucz 1994) generally have difficulties reproducing broad-band colors because of the complicated opacity calculations in the near-IR. Empirical libraries based predominantly on bright and nearby Milky Way stars (Kleinmann & Hall 1986; Lançon & Rocca-Volmerange 1992; Wallace

[1] Present address: Departamento de Astrofísica Molecular e Infrarroja, IEM, Consejo Superior de Investigaciones Científicas, Serrano 113b, 28006 Madrid, Spain

& Hinkle 1996, 1997; Meyer et al. 1998; Wallace et al. 2000) are limited to near solar metallicity. At the same time, realistic galaxy modeling requires metallicities ranging from [Fe/H]=−1.76 for the most metal-poor galaxy known I Zw 18 (Aloisi et al. 2003), to supersolar values, measured for at least for some giant elliptical galaxies (Casuso et al. 1996).

The properties of the most prominent near-IR spectral libraries available in the literature are summarized in Table 1. For a review of the earlier work see Merrill & Ridgway (1979). This summary shows that despite the sizable quantity of available stellar spectra, up until now there was no uniform near-IR dataset with high signal-to-noise and resolution, covering the entire range of spectral classes, luminosity, and metallicity necessary to carry out evolutionary population synthesis in the near-IR. The deficit of some types of stars such as metal-poor super giants is understandable in the context of the Milky Way star formation history, but the lack of many other types is rectifiable. We concentrate on metal features that have equivalent widths in a typical starburst galaxy larger than 1Å – as they can be measured reliably in spectra with signal-to-noise ratios of ∼30-50 (Engelbracht 1997).

A second application of our library, albeit no less important, is the analysis of individual stars hidden behind $A_V \geq 10$ mag of visual extinction. A typical case for such a population is represented by the Arches cluster member starss in the Galactic Center region (Nagata et al. 1993).

Here we describe the observations and the sample of an empirical near-IR stellar library that is designed to meet the requirements of population synthesis. The main advantage in comparison with previous work is the expanded metallicity coverage. We also present a few diagnostics methods to derive parameters of individual stars. The evolutionary population model will be published in a subsequent paper. The next section describes the observations and the data reduction technique. Sec. 3 summarizes the sample selection. Spectral indices are defined in Sec. 4, and some diagnostic applications for parameters of individual stars are considered in Sec. 5. In Sec. 6. we give the summary.

2. Observations and Data reduction

The near-IR spectra were taken from 1995 to 1999 mainly at the Steward Observatory 2.3m Bok telescope on Kitt Peak. Some stars were observed at the original 4.5m MMT and at the Steward Observatory 1.55m Kuiper telescope. We used FSpec (Williams et al. 1993), a cryogenic long slit near-IR spectrometer utilizing a NICMOS3 256x256 array (Kozlowski et al. 1993). The majority of the stars were observed with a 600 lines mm^{-1} grating, corresponding to a spectral resolution R≈2000-3000. This is the highest useful spectral resolution for studies of stellar populations in external galaxies where the intrinsic velocity dispersion smooths out the integrated spectra. The rest were observed with a 300 lines mm^{-1} grating and R≈1000-1500. The slit widths were 2.4 arcsec at the 2.3m, 1.2 arcsec at the MMT, and 3.6 arcsec at the 1.55m. The plate scales were 1.2, 0.6, and 1.8 arcsec pixel^{-1}, respectively. The limited physical size of the near-IR array required the acquisition of spectra at 10-12 grating positions, corresponding to different central wavelengths (λ_c) to cover the entire H and K atmospheric windows with sufficient overlap. Usually, one of the following two combinations of λ_c was used: 1.54, 1.62, 1.70, 2.06, 2.13, 2.19, 2.245, 2,31, 2.37, 2.42 μm, or 1.50, 1.57, 1.64, 1.71, 2.05, 2.10, 2.15, 2.20, 2.25, 2.30, 2.35, 2.40 μm. The log of observations is given in Table 2.

The observing strategy for a single setting included nodding the telescope to obtain spectra at 4 (at the MMT) or 6 (at the 2.3m and 1.55m telescopes) different positions along the slit, and integrating at each position for $3-20$ seconds, depending on the apparent brightness of the object and the sky background. This was necessary in order to: (i) carry out the sky emission subtraction and account for the sky background variations by having a sky taken just before and after the science exposures; (ii) improve the pixel sampling, flat fielding, and bad pixel correction by having the object placed on multiple positions on the array.

Next, we repeated the same procedure for a standard star at similar airmass (airmass difference $\leq$0.1-0.15) to correct for the atmospheric absorption. Then we changed the grating setting, obtained a sequence of $4-6$ spectra of the standard, moved the telescope back to the object, and

repeated the same procedure at the new grating setting. Occasionally, if two or three target stars were available nearby on the sky, we increased the observing efficiency by using the same telluric standard for all of them.

The spectra were reduced using *IRAF*[2] tasks written specifically for FSpec. An average of the sky backgrounds taken immediately before and after each object was subtracted to remove simultaneously the sky emission lines, and the dark current and bias level. Dark-subtracted illuminated dome flats taken at the same central wavelengths as the science exposures were applied to correct for pixel-to-pixel variations. The known bad pixels were masked out. Object images were shifted (using centroid fitting across the continuum), and median combined to produce a single two-dimensional spectrum. The large number of object images allowed us to reject any remaining bad pixels and cosmic rays. One-dimensional spectra were extracted by fitting a polynomial of order 3-5 to the continuum in the two-dimensional image with the *IRAF* task *apall*. The spatial width of the extraction apertures was usually 3-5 pixels, depending on the scale and the seeing.

In most cases the object spectra were divided by spectra of solar analog stars observed at the same airmass, and then multiplied by the solar spectrum (Livingston & Wallace 1991) to remove the effects of the photospheric absorption (Maiolino, Rieke & Rieke 1996). The standard stars were not always exactly G2 dwarfs (usually ranging from F8 V to G3 V), and the true shape of the continuum had to be restored by multiplying the spectra by the ratio of black bodies with the standard star and solar effective temperatures. In the cases we chose nearby A stars for telluric standards as an alternative of the solar analogs, we multiplied by another A star spectrum, already corrected for the photospheric absorption with a G2 V star. If an A type standard was used to correct only a K-band spectrum, we removed the Brγ feature by interactively fitting and subtracting a Gaussian with the task *splot*. We carried out the wavelength calibration using OH airglow lines (Oliva & Origlia 1992) complemented if necessary with Ne-Kr lamp spectra.

The spectrum at each individual setting was divided by second or third order polynomial continuum fits and combined with the rest of the settings to construct a single HK spectrum. Finally, we multiplied the spectrum by a black body with stellar effective temperature corresponding to the spectral type (Schmidt-Kaler 1982; Straižys 1992). Unfortunately, the normalization procedure removes the broad vapor absorption features in the coolest stars but this loss is unavoidable because the spectral extent of a single setting is only $0.075 - 0.095\,\mu$m and does not provide sufficient coverage for a reliable estimate of the continuum shape. Furthermore, in many cases the true continuum shape was distorted by the imperfect spectral type match of the telluric standards, as discussed above. The deviation between the constructed continuum shape and the real one is most severe for late M stars, where the molecular absorption is the strongest. A possible way to alleviate this problem completely is to impose on our spectra empirical continuum shapes taken from lower resolution spectra (Lançon & Rocca-Volmerange 1992; Lançon & Wood 2000). We intend to explore this avenue in the future.

The error analysis of spectra that consist of "pieces" taken at different times, and often on different nights, is particularly complicated because of the large variations of the signal-to-noise ratio (S/N) across the individual spectra. The uncertainties are dominated by systematic errors due to: (i) sky emission and transparency variations with wavelength, and (ii) temporal changes in the observing conditions. An example is given in Fig. 1, where the difference between the "final" spectra of two different K3 III stars with near solar metallicity is shown. The difference Δ has been divided by the average of the two spectra. The inset shows the distribution of these differences. Their average difference $<\Delta>$ is statistically indistinguishable from zero, and the value of the standard deviation σ suggests that each spectrum has an average S/N$\sim$50. At the same time, the photon statistics suggests S/N$\sim$150. The inconsistency is largely due to the variation of the sky background and transmission. Therefore, a single signal-to-noise ratio does not represent well the quality of the data. Furthermore, the measurements of individual features of interest include additional system-

[2]IRAF is distributed by the National Optical Astronomy Observatories, which are operated by the Association of Universities for Research in Astronomy, Inc., under cooperative agreement with the National Science Foundation.

atic uncertainties, such as the continuum placement during the continuum normalization, and differences between the stars used for the telluric correction and the Sun.

The best technique to estimate the actual signal-to-noise ratio is to measure the noise locally over a "clean" continuum region near the spectral feature of interest. We recommend this method for applications concerning parameters of individual stars. Our study shows that for statistical work the uncertainties of indices can be approximated as $\sigma(Index) = 0.2 \times Index$, with a lower limit of $\sigma(Index) = 0.02$ mag. Representative subsets of our spectra are shown in Fig. 2, 3, 4, and 5.

3. Sample Selection and Stellar Parameters

We have assembled an IR spectral library of 218 stars. The majority of them have photospheric parameters available from the literature. The main criterion to include various types of stars was to populate the *effective temperature – surface gravity – abundance* space necessary to model the stellar populations of starburst galaxies. Special attention was paid to observing red supergiants, which dominate the near-IR flux of these galaxies.

The largest fraction of stars in our library was selected from the Lick group sample (Worthey et al. 1994), assuring that they have high quality optical spectra and known spectral type, surface gravity, and metallicity. However, the Lick library was aimed at modeling galaxies with old stellar populations – ellipticals and bulges of spirals, – and therefore, is mainly composed of giants and dwarfs. We observed most red giants from their sample, and supplemented this set with super-metal rich stars from the Baade's Window region from McWilliam & Rich (1994) to expand their metallicity range. Next, we selected red supergiant stars from White & Wing (1978) and Luck & Bond (1989), to assure good coverage of the stars that dominate the stellar populations of galaxies with ages of 7-12 Myr – the so-called red-supergiant-phase. In addition, we observed various stars with known metal abundances from the catalog of Cayrel de Strobel et al. (1997). The distribution of our stars on the surface gravity $\log g$ versus effective temperature $T_{\rm eff}$ relation is shown in Fig. 6.

The photospheric data for the program stars are summarized in Table 3. About half of them (111 out of 218 stellar metallicities) were already available from Faber et al. (1985), Gorgas et al. (1993), and Worthey et al. (1994). The last work offers recalculated stellar parameters based on their own spectral line measurements and calibrations. To ensure that our system is as close as possible to theirs, we used these new estimates when available. In addition, we carried out an extensive literature search for photospheric data for the rest of our program stars. Our main source was the catalog of [Fe/H] determination of Cayrel de Strobel et al. (1997) which contains all metallicity estimates in the literature up to 1995. Naturally, this is an inhomogeneous compilation. In an effort to "homogenize" the data as much as possible, – at least in terms of abundance estimate methods – we used spectroscopic determinations when possible. Only did we use metallicities based on narrow band photometry when these were the only estimates available in the literature. Broad-band photometry based metallicities were adopted for six dwarf stars with no other measurements.

We made some assumptions when no photospheric parameters could be found in the literature: (i) solar metallicity was adopted for supergiants in the Galactic disk, and (ii) [Fe/H]=−0.21 was adopted for all bulge stars, following (Ramírez et al. 2000b). We neglect the 0.3 dex of metallicity dispersion in the bulge, until individual estimates become available. We included in the table some color information – the reddening corrected $(V-K)_0$ – for stars with unknown spectral class.

The metallicities as a function of the luminosity class for stars in our library are shown in Fig. 7. The giants show the largest [Fe/H] spread by far. The supergiants suffer from a pure astrophysical constraint: the massive metal poor stars from Population II (and possibly III) in our Galaxy exploded as supernovae a long time ago. The Magellanic Clouds offer a possibility to complement the library with some supergiants with 1/5 to 1/20 of the solar metallicity (Luck et al. 1998; Hill 1999). Obtaining such spectra is forseen in the next papers of this series.

4. Index Definitions

Some spectral features in the near-IR have been observed and measured, and suitable spectral indices have already been defined by Kleinmann & Hall (1986), Origlia, Moorwood & Oliva (1993), Doyon, Joseph & Wright (1994), and Ali et al. (1995). We adopted their definitions for compatibility, with two modifications. First, for the NaI and CaI indices of Ali et al. (1995) we used only the two nearest continuum bands. Second, for the CO index of Doyon, Joseph & Wright (1994) we carried a polynomial, rather than a power-law, fit to the continuum. Experiments show that both these changes produce no significant effects, within the errors.

Our spectra do not always span the wavelength range of the original photometric CO index of Frogel et al. (1978), and we were forced to measure only narrow spectral indices, including the one defined by Ivanov et al. (2000). The latter is somewhat intermediate between the narrow and broad CO indices, which makes it less sensitive to variations of the photospheric transmission. It provides better signal-to-noise than the narrower spectroscopic indices.

Finally, we defined new indices for atomic lines that had not been measured before, or where the previous definitions could be affected by the loss of the true continuum shape as discussed above, for instance, the indices defined by Kleinmann & Hall (1986) where the continuum bands are very far apart. All definitions are summarized in Table 4, and the bandpasses are shown in Fig. 8. The measured indices for the library stars are given in Table 5. The gaps in the table are due to incomplete spectral coverage.

All indices are in magnitudes:

$$\mathrm{Index} = -2.5 \times \log_{10}(\mathrm{I_{line}}/\mathrm{I_{continuum}}) \qquad (1)$$

where $\mathrm{I_{line}}$ is the flux in the line band, normalized by the band width, and $\mathrm{I_{continuum}}$ is linear interpolation of the continuum flux at the line wavelength. An exception are the CO bands for which $\mathrm{I_{continuum}}$ is the band width normalized flux in the continuum pass band.

5. Diagnostics of Individual Stars

5.1. Stellar Effective Temperature Indicators

Many near-IR spectral features are good indicators of the stellar effective temperature ($\mathrm{T_{eff}}$) by themselves, e.g., the CO bands, and the NaI, CaI indices (Kleinmann & Hall 1986). Fig. 9 shows the behavior of all measured features as function of $\mathrm{T_{eff}}$. To minimize metallicity effects we only plot stars with $-0.10 \leq$[Fe/H]$\leq +0.10$. The CO bands, Brγ, Na and Ca show stronger temperature dependence than for instance Mg, Fe and Si. This behavior has been demonstrated before (Kleinmann & Hall 1986; Ali et al. 1995; Förster-Schreiber 2000).

Some line ratios, for instance EW(CO 1.62)/EW(SiI 1.59) (Origlia, Moorwood & Oliva 1993; Dallier, Boisson & Joly 1996; Förster-Schreiber 2000), are better temperature indicators than individual lines because the division cancels out any additional luminosity, metallicity, or reddening effects. Based on the indices of 109 stars from our sample (Fig. 10) we find the following relation for giants and supergiants with $\mathrm{T_{eff}} \leq 5000$ K:

$$(\mathrm{CO\,1.62}-\mathrm{SiI\,1.59}) = (2.79\pm0.19)-(0.77\pm0.05)\times\log \mathrm{T_{eff}} \qquad (2)$$

Here we used the index definitions of Origlia, Moorwood & Oliva (1993). The root-mean-square (hereafter, r.m.s.) of the relation is 0.03 mag, which corresponds to ∼300 K for the inverse equation, close to the typical observational errors of 0.02 mag. From indices of 23 dwarfs and subgiants, again with $\mathrm{T_{eff}} \leq 5000$ K:

$$(\mathrm{CO\,1.62}-\mathrm{SiI\,1.59}) = (0.65\pm0.20)-(0.19\pm0.05)\times\log \mathrm{T_{eff}} \qquad (3)$$

where the r.m.s is 0.02 mag, corresponding to ∼800 K. The slopes of the relations are significantly different, and the loci of the two groups overlap only for hot stars where both spectral features are weak and the relative errors increase.

We derived similar relations using the 1.50 μm MgI feature. For 107 giants and supergiants:

$$(\mathrm{CO\,1.62}-\mathrm{MgI\,1.50}) = (2.34\pm0.21)-(0.65\pm0.06)\times\log \mathrm{T_{eff}} \qquad (4)$$

The CO index is defined by Origlia, Moorwood & Oliva (1993) and the MgI index is defined in this work. The r.m.s. is 0.03 mag or ∼350 K. For 23

dwarfs and sub-giants:

$$(\mathrm{CO\,1.62}-\mathrm{MgI\,1.50}) = (1.13\pm0.59)-(0.34\pm0.16)\times\log\mathrm{T_{eff}} \quad (5)$$

with r.m.s. of 0.06 mag or ∼1500 K. The relations for dwarfs and sub-giants are worse than for giants and supergiants because of both weaker spectral lines and systematically fainter targets. Note that even though we have not restricted the abundances, the majority of stars used to derive the equations above have near-solar metallicities ($-0.2\leq$[Fe/H]$\leq+0.2$) and abundance ratios.

5.2. Two-dimensional Spectral Classification – Luminosity Class Indicators

The two-dimensional spectral classification requires an indicator for the intrinsic luminosity of the stars. Kleinmann & Hall (1986) demonstrated that Na, Ca and Brγ can be used to discriminate between stars of different luminosity classes (see their Fig. 7). We verified their result, excluding the Brγ index (Fig. 11) to minimize the uncertainties related to the removal of the intrinsic Brγ absorption in the telluric standards (Sec. 3). The (super)giant versus dwarf separation is relatively small, compared with the typical observational uncertainties. The situation improves if we constrain the sample only to metal rich stars with [Fe/H]≥-0.5 (bottom panel), minimizing the relative errors. Clearly, this diagnostic relationship imposes a high demand on the data quality.

Ramírez et al. (1997) proposed to use the log{EW(CO 2.29)/[EW(NaI 2.21)+EW(CaI 2.26)]} ratio plotted against $\mathrm{T_{eff}}$ to separate giants from dwarfs (see their Fig. 11). Our data confirm this result (Fig. 12, bottom left), even for higher $\mathrm{T_{eff}}$ than Ramírez et al. (1997) because of the improved S/N and spectral resolution. We obtain similar separation with Mg features (Fig. 12, top left). This methods use a physical quantity – $\mathrm{T_{eff}}$ – that requires some calibration to be derived from observables such as $(V-K)_0$ or some spectral feature. To avoid this additional step, we combined the two ratios – log{EW(CO 2.29)/[EW(NaI 2.21)+EW(CaI 2.26)]} and log{EW(CO 1.62)/[EW(MgI 1.50)+EW(MgI 1.71)]}, – and found that we can still achieve separation for most of the stars.

The signal-to-noise ratio needed to use the diagnostics discussed here depends on the temperature of the stars. It is safe to assume that S/N∼30 is necessary for K5-M stars, and it increases up to 50 for early K stars. The lines become too weak to implement these techniques for stars with effective temperatures hotter than $4500-4800$ K. An additional limitation comes from the metal abundance – it is more difficult to separate stars of different luminosity class with low metallicity than with high metallicity, because in the former the lined are weaker, and the relative uncertainties are higher. However, our library does not offer sufficient abundance range to quantify this effect.

6. Summary

We have assembled a library of moderately high-resolution (≈2000-3000) H (1.6 μm) and K (2.2 μm) spectra of 218 red stars, mostly supergiants and giants. The majority of these stars have well-known photospheric parameters from high-resolution optical spectroscopy. These stars dominate the near-IR emission in both starburst and elliptical galaxies. Our library covers a range of effective temperatures, and metal abundances from [Fe/H]~-2.2 to $+0.3$. This library will offer a unique opportunity to study directly the most obscured stellar populations in starburst galaxies, as well as in the center of the Milky Way.

Although the main motivation behind the creation of this library is the study of unresolved extragalactic stellar populations, the obtained spectra can be used to derive parameters of individual stars. We calibrated some line ratios as indicators of the stellar effective temperature. Finally, we demonstrated how some diagnostic relationships can distinguish (super)giants from dwarf stars.

This research has made use of the SIMBAD database, operated at CDS, Strasbourg, France. The authors were supported by NSF grant AST 95-29190. We are grateful to the anonymous referee for the suggestions that helped to improve the paper.

REFERENCES

Abt, H.A. 1981, ApJS, 45, 437

Ali, B., Carr, J.S., Depoy, D.L., Frogel, J.A., Sellgren, K., 1995, AJ, 110, 2415

Aloisi, A., Savaglio, S., Heckman, T.M., Hoopes, C.G., Leitherer, C., & Sembach, K.R. 2003, ApJ, in print

Alonso, A., Arribas, S., & Martinez-Roger, C., 1994, A&AS, 107, 365

Alvarez, R., Lançon, A., Plez, B., Wood, P.R., 2000, A&A, 353, 322

Appenzeller, I. 1967, PASP, 79, 102

Barbier, M. 1962, Journal des Observateurs, 45, 57

Barbier, M. 1968, Publ. Obs. Haute-Provence, 9, 38

Bell, R.A., & Gustafsson, B., 1989, MNRAS, 236, 653

Bidelman, W.P. 1957, PASP, 69, 326

Blanco, V.M., McCarthy, M.F., & Blanco, B.M. 1984, AJ, 89, 636

Blanco, V.M. 1986, AJ, 91, 290

Brown, J.A., Sneden, C., Lambert, D.L., & Dutchover Jr., E. 1989, ApJS, 71, 293

Bruzual, G.A., & Charlot, S., 1993, ApJ, 405, 538

Casuso, E., Vazdekis, A., Peletier, R.F., & Beckman, J.E. 1996, ApJ, 458, 533

Cayrel de Strobel, G., Soubiran, C., Friel, E.D., Ralite, N., François, P., 1997, A&AS, 124, 299

Cayrel de Strobel, G., Soubiran, C., Ralite, N. 2001, A&A, 373, 159

Cowley, A. 1972, AJ, 77, 750

Cowley, A., Cowley, C., Jaschek, M., Jaschek, C. 1969, AJ, 74, 375

Dallier, R., Boisson, C. & Joly, M., 1996, A&AS, 116, 239

Di Benedetto, G.P., 1998, A&A, 339, 858

Doyon, R., Joseph, R.D., & Wright, G.S., 1994 ApJ, 421, 101

Dumm, T., & Schild, H., 1998, NewA, 3, 137

Eaton, J.A. 1995, AJ, 109, 1797

Eggen, O.J. 1996, AJ, 111, 466

Eggen, O.J. 1998, AJ, 115, 2397

Eggen, O.J., & Stokes, N.R., 1970, ApJ, 161, 199

Engelbracht, C.W., 1997, Ph.D. Thesis, The University of Arizona, Tucson

Faber, S.M., Friel, E.D., Burstein, D., & Gaskell, C.M., 1985, ApJS, 57, 711

Fehrenbach, C., Rebeirot, E., Petit, M., Peyrin, Y., & Monvoisin, C. 1962, Journal des Observateurs, 45, 349

Feltzing S. & Gustafsson, B., 1998, A&A, 129, 237

Fernie, J.D., 1959, ApJ, 130, 610

Förster-Schreiber, N.M., 2000, AJ, 120, 2089

Frogel, J.A., Persson, S.E., Aaronson, M., & Matthews, K., 1978, ApJ, 220, 75

Garmany, C.D., & Stencel, R.E., 1992, A&AS, 94, 211

Ginestet, N. & Carquillat, J.M. 2002, ApJS, 143, 513

Gorgas, J., Faber, S.M., Burstein, D., Gonzalez, J.J., Courteau, S., & Prosser, C., 1993, ApJ, 86, 153

Gray, R.O., Napier, M.C., & Winkler, L.I. 2001, AJ, 121, 2148

Greenstein, J.L., & Keenan, P.C. 1958, ApJ, 127, 172

Halliday, I. 1955, ApJ, 122, 222

Hanson, M.M., Conti, P.S., Rieke, M.J., 1996, ApJS, 107, 281

Harlan, E.A. 1969, AJ, 74, 916

Haywood, M. 2001, MNRAS, 325, 1365

Henry, T.J., Kirkpatrick, J.D., & Simons, D.A. 1994, AJ, 108, 1437

Hicks, E.K., Malkan, M.A., Teplitz, H.I., Sugai, H., Guichard, J., 2000, AAS, 197.4408

Hill, V., 1999, A&A, 345, 430

Houk, N., & Smith-Moore, M. 1988, Michigan Spectral Survey, Ann Arbor, Dep. Astron., Univ. Michigan, 4

Humphreys, R.M., 1970, AJ, 75, 602

Ivanov, V.D., Rieke, G.H., Groppi, C.E., Alonso-Herrero, A., Rieke, M.J., & Engelbracht, C.W., 2000, ApJ, 545, 190

Johnson, H.L., 1966, ARA&A, 4, 193

Johnson, H.J. & Mèndez, M.E., 1970, AJ, 75, 785

Johnson, H.J. & Morgan, W.W. 1953, ApJ, 117, 313

Joy, A.H. & Abt, H.A. 1974, ApJS, 28, 1

Joyce, R.R., 1998, AJ, 115, 2059

Keenan, P.C., & Keller, G. 1953, ApJ, 117, 241

Keenan, P.C., & McNeil, R.C. 1989, ApJS, 71, 245

Kirkpatrick, J.D., Kelly, D.M., Rieke, G.H., Liebert, J., Allard, F., Wehrse, R., 1993, ApJ, 402, 643

Kirkpatrick, J.D., Henry, T.J., & McCarthy, D.W., Jr.. 1991, ApJS, 77, 417

Kleinmann, S.G., & Hall, D.N.B., 1986, ApJS, 62, 501

Kozlowski, L.J., Kadri, V., Cooper, D.E., Bailey, R.B., Bui, D.Q., & Stephenson, D.M. 1993, Proc. SPIE 1946, Infrared Detectors and Instrumentation, 149

Kurucz, R., 1994, Solar abundance model atmospheres for 0,1,2,4,8 km/s. Kurucz CD-ROM No. 19. Cambridge, Mass.: Smithsonian Astrophysical Observatory, 1994.

Lançon, A. & Rocca-Volmerange, B., 1992, A&AS, 96, 593

Lançon, A. & Wood, P.R., 2000, A&AS, 146, 217

Lee, T.A., 1970, ApJ, 162, 217

Leggett, S.K., Allard, F., Berriman, G., Dahn, C.C., & Hauschildt, P.H., 1996, ApJS, 104, 117

Leggett, S.K., Allard, F., Dahn. C., Hauschildt, P.H., Kerr, T.H., & Rayner, J., 2000, ApJ, 535, 965

Leitherer, C., Schaerer, D., Goldader, J.D., Delgado, R.M.G., Robert, C., Kune, D.F., de Melo, D.F., Devost, D. & Heckman, T., 1999, ApJS, 123, 3

Livingston, W. & Wallace, L., 1991, An Atlas of the Solar Spectrum in the Infrared from 1850 to 9000 cm^{-1} (1.1 to 5.4 μm), N.S.O., Technical Report # 91-001, National Solar Observatory, National Optical Astronomical Observatories, Tucson, AZ, U.S.A.

Lloyd Evans, T. 1976, MNRAS, 174, 169

Luck, R.E. & Bond, H.E., 1989, ApJS, 71, 559

Luck, R.E., Moffet, T.J., Barnes, T.G. III, Gieren, W.P., 1998, AJ, 115, 605

Lutz, T.E., & Lutz, J.H. 1977, AJ, 82, 431

Maiolino, R., Rieke, G.H., & Rieke, M.J., 1996, AJ, 111, 537

McWilliam, A. & Rich, R.M., 1994, ApJS, 91, 749

Merrill, K.M., & Ridgway, S.T., 1979, ARA&A, 17, 9

Meyer, M.R., Edwards, S., Hinkle, K.H., & Strom, S.E., 1998, ApJ, 508, 397

Morgan, W.W., Harris, D.L., & Johnson, H.L. 1953, ApJ, 118, 92

Nassau, J.J., & van Algabada, G.B. 1947, ApJ, 106, 20

Nagata, T., Hyland, A.R., Straw, S.M., Sato, S., Kawara, K. 1993, ApJ, 406, 501

Oliva, E., & Origlia, L. 1992, A&A, 254, 466

Origlia, L., Moorwood, A.F.M., & Oliva, E., 1993, A&A, 280, 536

Preston, G.W., Bidelman, W.P. 1956, PASP, 68, 533

Ramírez, S.V., DePoy, D.L., Frogel, J.A., Sellgren, K., & Blum, R.D., 1997, AJ, 113, 1411

Ramírez, S.V., Sellgren, K., Carr, J.S., Balachandran, S.C., Blum, R., Terndrup, D.M., Steed, A. 2000a, ApJ, 537, 205

Ramírez, S.V., Stephens, A.W., Frogel, J.A., & DePoy, D.L. 2000b, AJ, 120, 833

Rieke, G.H., Lebofsky, M.J., Thompson, R.I., Low, F.J., & Tokunaga, A.T., 1980, ApJ, 238, 24

Rieke, G.H., & Lebofsky, M.J. 1985, ApJ, 288, 618

Rieke, G.H., Locken, K., Rieke, M.J., & Tamblyn, P., 1993, ApJ, 412, 99

Roman, N.G. 1952, ApJ, 116, 122

Roman, N.G. 1955, ApJS, 2, 195

Santos, N.C., Israelian, G., Mayor, M., Rebolo, R., & Udry, S. 2003, A&A, 398, 363

Schmidt-Kaler, T., 1982, in Landolt-Borstein, New Series, Group VI, vol. 2, ed. K. Schaifers & H.H. Voigt (Berlin: Springer-Verlag),1

Schmitt, J.L. 1971, ApJ, 163, 75

Sloan, G.C., & Price, S.D. 1998, ApJS, 119, 141

Straižys, V., 1992, Multicolor Stellar Photometry, Pachart Pub., Tucson, Arizona, U.S.A.

Taylor, B.J., 1991, ApJS, 76, 715

Taylor, B.J., 1999, A&A, 134, 523

Taylor, B.J., Spinrad, H., & Schweizer, F., 1972, ApJ, 173, 619

Upgren, A.R., & Staron, R.T. 1970, ApJS, 19, 367

van Belle, G.T., Lane, B.F., Thompson, R.R., Boden, A.F., Colavita, M.M., Dumont, P.J., Mobley, D.W., Palmer, D., Shao, M., Vasisht, G.X., Wallace, J.K., Creech-Eakman, M.J., Koresko, C.D., Kulkarni, S.R., Pan, X.P., & Gubler, J., 1999, AJ, 117, 521

van Dyck, H.M., van Belle, G.T. & Thompson, R.R., 1998, AJ, 116, 981

Vazdekis, A., 1999, ApJ, 513, 224

Wallace, L. & Hinkle, K., 1996, ApJS, 107, 312

Wallace, L. & Hinkle, K., 1997, ApJS, 111, 445

Wallace, L., Meyer, M.P., Hinkle, K., Edwards, S., 2000, ApJ, 535, 325

White, N.M. & Wing, R.F., 1978, ApJ, 222, 209

Williams, D.M., Thompson, C.L., Rieke, G.H., & Montgomery, E.F., 1993, S.P.I.E., 1946, 482

Worthey, G., 1994, ApJS, 95, 107

Worthey, G., Faber, S.M., Gonzalez, J.J. & Burstein, D., 1994, ApJS, 94, 687

Zakhozhaj V.A., & Shaparenko E.F., 1996, Kin. Fiz. Nebesn. Tel., 12, No, 2, 20

Zhou Xu, 1991, A&A, 248, 367

Table 1
Near-IR spectral libraries. This work is included for comparison.

Spectral Library Reference	λ μm	Sp. Type and Lum. Class range	No. Stars	Spectral Resolution
Johnson & Mèndez (1970)	1.2-2.5	A-M, I-V	32	550
Kleinmann & Hall (1986)	2.0-2.5	F-M, I-V	26	2500-3100
Lançon & Rocca-Volmerange (1992)	1.4-2.5	O-M, I-V	56	550
Origlia, Moorwood & Oliva (1993)	1.5-1.7	G-M, I-V	40	1500
Ali et al. (1995)	2.0-2.4	F-M, V	33	1380
Wallace & Hinkle (1996)	2.02-2.41	G-M, I-V	12	45000
Dallier, Boisson & Joly (1996)	1.57-1.64	O-M, I-V	37	1500-2000
Hanson, Conti & Rieke (1996)	2.0-2.4	O-B, I-V	180	800-3000
Ramírez et al. (1997)	2.19-2.34	K-M, III	43	1380,4830
Wallace & Hinkle (1997)	2.0-2.4	O-M, I-V	115	3000
Meyer et al. (1998)	1.5-1.7	O-M, I-V	85	3000
Joyce (1998)	1.0-2.5	K-M, III	29	500-1500
Förster-Schreiber (2000)	1.90-2.45	G-M, I-III	31	830,3000
Wallace et al. (2000)	1.05-1.34	O-M, I-V	88	3000
Lançon & Wood (2000)	0.5-2.5	K-M, I-III	77	1100
Hicks et al. (2000)	1.08-1.35	O-M, I-V	105	650
This work	1.48-2.45	G-M, I-V	218	2000-3000

Table 2
Log of spectroscopic observations.

Date (1)	Site (2)	Star (3)	Std. (4)	Sp.T. (5)	Gr. (6)	Range (7)
951209	61	S074439	S074506	A3 V	600	HK
951209	61	S060890	HR3348	A0 V	600	HK
951209	61	S027179	HR3592	A2 V	600	HK
951209	61	VYLeo	HR4244	A3 V	600	H
951210	61	S074175	HR0277	A2 V	600	HK
951210	61	S109474	HR0081	A0 V	600	HK
951210	61	S109471	HR0081	A0 V	600	HK
951210	61	S074883	HR0669	A1 V	600	2.30-2.40
951210	61	S080333	HR3481	A1 V	600	HK
951210	61	S098021	HR3481	A1 V	600	HK
951210	61	S098087	HR3481	A1 V	600	HK
951210	61	GL406	HR4244	A3 V	600	H,2.05-2.15
951211	61	GL905	HR0001	A1 V	600	2.20-2.40
951211	61	GL15NE	HR0001	A1 V	600	2.20-2.40
951211	61	GL15SW	HR0001	A1 V	600	2.20-2.40
951211	61	S074883	HR0669	A1 V	600	1.50-2.25
951213	61	GL905	HR0001	A1 V	600	1.50-2.15
951213	61	GL15NE	HR0001	A1 V	600	1.50-2.15
951213	61	GL15SW	HR0001	A1 V	600	1.50-2.15
951213	61	GL83-1	HR2578	A6 V	600	HK
951213	61	GL65AB	HR0451	A3 V	600	HK
951213	61	HR1324	HR1272	A3 V	600	HK
951213	61	GL166C	HR1272	A3 V	600	HK
951213	61	S116988	HR3406	A3 V	600	HK
951213	61	S116569	HR3406	A3 V	600	HK
951213	61	VYLeo	HR4244	A3 V	600	2.20-2.40
951213	61	GL402	HR4244	A3 V	600	2.20-2.40
951213	61	GL412A	HR4380	A2 V	600	2.05-2.30
951213	61	GL411	HR4380	A2 V	600	2.05-2.30
951214	61	GL866	HR8816	A0 V	600	HK
951214	61	HR8841	HR8816	A0 V	600	HK
951214	61	HR0617	HR0669	A1 V	600	2.25-2.40
951214	61	GL213	HR1819	A4 V	600	HK
951214	61	HR1907	HR1819	A4 V	600	HK
951214	61	GL206	HR1819	A4 V	600	HK
951214	61	HR3905	HR4041	A0 V	600	HK
951214	61	GL388	HR4041	A0 V	600	HK
951215	61	HR0617	HR0669	A1 V	600	1.50-2.20
951215	61	HR0867	HR0972	A1 V	600	HK
951215	61	HR1015	HR0972	A1 V	600	HK
951218	61	HR8795	HR8826	A5 V	600	HK
951218	61	HR8860	HR8837	A0 V	600	1.50-2.20
951218	61	HR8832	HR8837	A0 V	600	1.50-2.20
960301	61	HR3538	HR3314	A0 V	600	HK
960301	61	HR4299	HR4356	A0 V	600	HK
960301	61	HR4883	HR4738	A4 V	600	HK
960301	61	HR4954	HR4738	A4 V	600	HK
960301	61	S44383	HR5169	A1 V	600	HK
960302	61	HR3359	HR3314	A0 V	600	HK
960302	61	HR4069	HR4113	A4 V	600	HK
960302	61	HR4184	HR4113	A4 V	600	HK

Table 2—*Continued*

Date (1)	Site (2)	Star (3)	Std. (4)	Sp.T. (5)	Gr. (6)	Range (7)
960302	61	HR4932	HR4805	A1 V	600	2.35-2.40
960302	61	S119433	HR4805	A1 V	600	2.35-2.40
960505	61	HR4362	HR4357	A4 V	600	HK
960505	61	S082106	HR4357	A4 V	600	HK
960505	61	HR5072	HR5144	A1 V	600	H
960505	61	GL526	HR5144	A1 V	600	H
960505	61	HR5072	HR5010	F0 V	600	K
960505	61	GL526	HR5010	F0 V	600	K
960505	61	HR6242	HR6123	A5 V	600	HK
960505	61	S045933	HR6123	A5 V	600	HK
960505	61	HR7475	HR7546	A3 V	600	K
960505	61	H339034	HR7546	A3 V	600	K
960506	61	HR4496	HR4380	A2 V	600	HK
960506	61	HR4716	HR5142	A3 V	600	HK
960506	61	HR5019	HR4776	F2 V	600	HK
960506	61	HR5853	HR6093	F2 V	600	HK
960506	61	HR6014	HR6093	F2 V	600	HK
960506	61	HR6623	HR6324	A0 V	600	HK
960506	61	HR6418	HR6324	A0 V	600	HK
960506	61	HR6212	HR6324	A0 V	600	HK
960505	61	HR7475	HR7546	A3 V	600	H
960506	61	H339034	HR7546	A3 V	600	H
960506	61	HR8465	HR8585	A1 V	600	H
960506	61	S034529	HR8585	A1 V	600	H
960507	61	GL380	HR3799	A2 V	600	HK
960507	61	HR5270	HR5392	A5 V	600	HK
960507	61	HR5409	HR5392	A5 V	600	HK
960507	61	HR5594	HR5392	A5 V	600	HK
960507	61	GL570A	HR5570	F0 V	600	HK
960507	61	GL570B	HR5570	F0 V	600	HK
960507	61	NR6713	HR6629	A0 V	600	HK
960507	61	NR8465	HR8585	A1 V	600	K
960507	61	S034529	HR8585	A1 V	600	K
960508	61	GL328	HR3651	A0 V	300	HK
960508	61	GL338	HR3592	A2 V	300	HK
960508	61	GL352	HR3909	A1 V	300	HK
960508	61	GL381	HR3909	A1 V	300	HK
960508	61	GL382	HR3909	A1 V	300	HK
960508	61	GL402	HR4227	A2 V	300	HK
960508	61	GL406	HR4227	A2 V	300	HK
960508	61	GL411	HR4422	A2 V	300	HK
960508	61	HR4375	HR4422	A2 V	300	HK
960508	61	GL436	HR4738	A4 V	300	HK
960508	61	S028414	HR5142	A3 V	300	HK
960508	61	HR5553	HR5386	A0 V	600	HK
960508	61	HR5235	HR5386	A0 V	600	HK
960508	61	HR6498	HR6629	A0 V	600	HK
960508	61	S122610	HR6629	A0 V	600	HK
960508	61	HR6752	HR6629	A0 V	600	HK
960508	61	HR8085	HR8028	A1 V	600	K
960508	61	HR8086	HR8028	A1 V	600	K
960509	61	HR4400	HR4356	A0 V	600	HK
960509	61	HR4418	HR4356	A0 V	600	HK

Table 2—*Continued*

Date (1)	Site (2)	Star (3)	Std. (4)	Sp.T. (5)	Gr. (6)	Range (7)
960509	61	HR5901	HR5774	A5 V	600	HK
960509	61	HR5800	HR5774	A5 V	600	HK
960509	61	HR5770	HR5870	A3 V	600	1.70
960509	61	HR6092	HR5874	A5 V	600	1.70
960509	61	HR6588	HR6509	A4 V	600	1.70
960509	61	HR6353	HR6534	A5 V	600	1.70
960509	61	HR5932	HR6123	A5 V	600	HK
960509	61	HR6146	HR6123	A5 V	600	HK
960509	61	HR7009	HR7051	A4 V	600	HK
960509	61	HR7139	HR7051	A4 V	600	HK
960509	61	HR8085	HR8028	A1 V	600	H
960509	61	HR8086	HR8028	A1 V	600	H
960510	61	HR4666	HR4738	A4 V	600	HK
960510	61	HR4668	HR4738	A4 V	600	HK
960510	61	HR5600	HR5676	A2 V	600	HK
960510	61	HR5616	HR5676	A2 V	600	HK
960510	61	HR6364	HR6457	A2 V	600	HK
960510	61	HR7063	HR6930	A3 V	600	HK
960510	61	HR7957	HR7619	A4 V	600	HK
960510	61	S033232	HR7619	A4 V	600	HK
960625	90	BMB239	HR6836	G0 V	600	2.20-2.40
960625	90	BMB181	HR6836	G0 V	600	2.20-2.40
960625	90	TLE205	HR6836	G0 V	600	2.20-2.40
960625	90	BMB289	HR6836	G0 V	600	2.20-2.40
960625	90	BMB194	HR6836	G0 V	600	2.20-2.40
960625	90	BMB39	HR6836	G0 V	600	2.20-2.40
960625	90	C669	HR0005	G5 V	600	2.10-2.20
960625	90	C501	HR0005	G5 V	600	2.10-2.20
960625	90	C468	HR0005	G5 V	600	2.10-2.20
960625	90	C971	HR0005	G5 V	600	2.10-2.20
960626	90	BMB239	HR6836	G0 V	600	2.10-2.15
960626	90	BMB181	HR6836	G0 V	600	2.10-2.15
960626	90	TLE205	HR6836	G0 V	600	2.10-2.15
960626	90	BMB289	HR6836	G0 V	600	2.10-2.15
960626	90	BMB194	HR6836	G0 V	600	2.10-2.15
960626	90	BMB39	HR6836	G0 V	600	2.10-2.15
960626	90	HR8085	HR8028	A1 V	600	2.10-2.15
960626	90	HR8086	HR8028	A1 V	600	2.10-2.15
960626	90	C669	HR0005	G5 V	600	2.25-2.40
960626	90	C501	HR0005	G5 V	600	2.25-2.40
960626	90	C468	HR0005	G5 V	600	2.25-2.40
960626	90	C971	HR0005	G5 V	600	2.25-2.40
960627	90	GL626	HR5853	G5 V	300	K
960627	90	HR6156	HR5853	G5 V	300	K
960627	90	S045933	HR5853	G5 V	300	K
960627	90	HR6014	HR5853	G5 V	300	K
960627	90	HR5859	HR5853	G5 V	300	K
960627	90	GL644	HR5853	G5 V	300	K
960627	90	HR6033	HR5853	G5 V	300	K
960627	90	BMB285	HR6836	G0 V	300	HK
960627	90	B133	HR6836	G0 V	300	HK
960627	90	BMB179	HR6836	G0 V	300	HK
960627	90	BMB87	HR6836	G0 V	300	HK

Table 2—*Continued*

Date (1)	Site (2)	Star (3)	Std. (4)	Sp.T. (5)	Gr. (6)	Range (7)
960627	90	BMB142	HR6836	G0 V	300	HK
960627	90	HR7162	HR6836	G4.5 V	300	K
960627	90	HR7102	HR6836	G4.5 V	300	K
960627	90	HR7368	HR6836	G4.5 V	300	K
960627	90	GL725B	HR6836	G4.5 V	300	K
960627	90	GL725A	HR6836	G4.5 V	300	K
960627	90	HR7251	HR6836	G4.5 V	300	K
960627	90	S031745	HR6836	G4.5 V	300	K
960627	90	HR7957	HR6836	G4.5 V	300	K
960627	90	GL752B	HR6836	G4.5 V	300	K
960627	90	GL752A	HR6836	G4.5 V	300	K
960627	90	HR7332	HR6836	G4.5 V	300	K
960627	90	S126068	HR6836	G4.5 V	300	K
960627	90	HR8086	HR6836	G4.5 V	300	K
960627	90	HR8085	HR6836	G4.5 V	300	K
960627	90	HR8028	HR6836	G4.5 V	300	K
960627	90	C415	HR0005	G5 V	300	K
960627	90	C575	HR0005	G5 V	300	K
960627	90	C676	HR0005	G5 V	300	K
960627	90	C857	HR0005	G5 V	300	K
960627	90	C875	HR0005	G5 V	300	K
960627	90	C897	HR0005	G5 V	300	K
960628	90	S045933	HR6156	A1 V	300	K
960628	90	GL625	HR6156	A1 V	300	K
960628	90	S122610	HR6629	A0 V	300	HK
960628	90	S031745	HR7251	A0 V	300	H
960628	90	GL673	HR6629	A0 V	300	HK
960628	90	HR6752	HR6629	A0 V	300	HK
960628	90	GL725A	HR7251	A0 V	300	H
960701	90	GL380	HR3799	A2 V	300	K
960701	90	GL411	HR4380	A2 V	300	K
960701	90	GL412A	HR4380	A2 V	300	K
960701	90	HR4785	HR5142	A3 V	300	K
960701	90	S028414	HR5142	A3 V	300	K
960701	90	HR5072	HR5144	A1 V	300	K
960701	90	GL526	HR5144	A1 V	300	K
960701	90	BMB239	HR6836	G0 V	600	1.65-1.70
960701	90	BMB181	HR6836	G0 V	600	1.65-1.70
960701	90	TLE205	HR6836	G0 V	600	1.65-1.70
960701	90	BMB289	HR6836	G0 V	600	1.65-1.70
960701	90	BMB194	HR6836	G0 V	600	1.65-1.70
960701	90	BMB39	HR6836	G0 V	600	1.65-1.70
961030	90	N188II72	HR0240	A4 V	600	HK
961030	90	N188I105	HR0240	A4 V	600	HK
961031	90	S105082	HR7390	A0 V	600	HK(−2.40)
961031	90	HR8841	HR8840	A3 V	600	HK(−2.40)
961031	90	HR8924	HR8840	A3 V	600	HK(−2.40)
961031	90	N188-359	HR0240	A4 V	600	HK(−2.40)
961031	90	N188-473	HR0240	A4 V	600	HK(−2.40)
961031	90	HR1726	HR1752	A1 V	600	HK(−2.40)
961031	90	HR1805	HR1752	A1 V	600	HK(−2.40)
970327	90	HR3905	HR3792	A3 V	600	HK
970327	90	HR4365	HR4437	G0 V	600	HK

Table 2—*Continued*

Date (1)	Site (2)	Star (3)	Std. (4)	Sp.T. (5)	Gr. (6)	Range (7)
970613	MM	M92III13	HR6469	F9 V	600	K
980405	90	HR3428	HR3510	G1 V	600	K(−2.42)
980405	90	HR4521	HR4439	G1 V	600	HK
980406	90	HR3428	HR3510	G1 V	600	1.62-1.70
980406	90	HR3905	HR3951	G3 V	600	1.50-2.19
980406	90	M3III28	HR4983	G0 V	600	1.50-2.19
980407	90	HR2503	HR2779	G0 V	600	2.24-2.42
980407	90	HR3905	HR3951	G3 V	600	2.24-2.42
980407	90	HR4287	HR4005	F6 V	600	2.24-2.37
980407	90	M3III28	HR4983	G0 V	600	2.24-2.37
980408	90	HR2289	HR2483	G0 V	600	2.02-2.32
980408	90	H77729	HR3563	F6 V	600	2.32
980408	90	HR4986	HR5011	G0 V	600	2.32
980408	90	M3III28	HR4983	G0 V	600	2.24
980408	90	S185981	HR6595	F6 V	600	2.20-2.32
980408	90	BMB289	HR6836	G0 V	600	2.19-2.24
980408	90	B+243902	HR7386	F7 V	600	2.32
980409	90	HR2289	HR2483	G0 V	600	H,2.37-2.42
980409	90	HR3428	HR3510	G1 V	600	2.42
980409	90	M3III28	HR4983	G0 V	600	2.06,2.24
980409	90	BMB289	HR6836	G0 V	600	H,2.19-2.24
980410	90	HR2854	HR2918	G0 V	600	HK
980410	90	H77729	HR3563	F6 V	600	1.54-62,K(−2.32)
980410	90	HR3994	HR4158	F7 V	600	HK
980410	90	HR4287	HR4005	F6 V	600	1.54-1.62
980410	90	M2III28	HR4983	G0 V	600	H
980410	90	HR5370	HR5346	G0 V	600	HK
980410	90	HR5829	HR5583	F8 V	600	HK
980410	90	S008274	HR5596	F9 V	600	HK
980410	90	BMB289	HR6836	G0 V	600	2.31-2.42
980603	90	HR4986	HR5011	G0 V	600	HK
980603	90	M5III3	HR5721	F0 V	600	1.54-1.62
980605	90	M5III3	HR5721	F0 V	600	2.06-2.24
980606	90	S119734	HR5011	G0 V	600	HK
980607	90	M13B786	HR6064	G1 V	600	K
980607	90	M71A6	HR7580	B9.5 V	600	2.13-2.42
980608	90	HR5366	HR5384	G2 V	600	HK
980608	90	HR5681	HR5968	G2 V	600	1.54-2.24
980608	90	BMB239	HR6836	G2 V	600	1.54
980608	90	BMB181	HR6836	G2 V	600	1.54
980608	90	TLE205	HR6836	G2 V	600	1.54
980608	90	BMB194	HR6836	G2 V	600	1.54
980608	90	BMB039	HR6836	G2 V	600	1.54
980608	90	BMB289	HR6836	G2 V	600	2.06-2.13
980608	90	M71A6	HR7580	B9.5 V	600	H
980608	90	M71A4	HR7580	B9.5 V	600	H
980609	90	HR5366	HR5384	G2 V	600	HK
980609	90	M5III3	HR5721	F0 V	600	1.62-70,2.31-2.37
980609	90	S185981	HR6595	F6 V	600	1.54-2.13,2.37-2.42
980609	90	H339034	HR7386	F7 V	600	HK(−1.71)
980609	90	BCCyg	HR7887	F0 V	600	2.24-2.42
980609	90	BICyg	HR7887	F0 V	600	2.24-2.42
980609	90	KYCyg	HR7887	F0 V	600	2.24-2.42

Table 2—*Continued*

Date (1)	Site (2)	Star (3)	Std. (4)	Sp.T. (5)	Gr. (6)	Range (7)
980610	90	HR5196	HR5019	G6 V	600	HK
980610	90	HR5582	HR5455	F5 V	600	HK(−1.70)
980610	90	HR5681	HR5968	G2 V	600	2.31-2.42
980610	90	M5III3	HR5721	F0 V	600	2.42
980611	90	M5III3	HR5721	F0 V	600	2.42
980611	90	M13B786	HR6064	G1 V	600	H
980611	90	HR2697	HR5581	F7 V	600	HK
980611	90	HR5947	HR5968	G2 V	600	HK
980611	90	M92XII8	HR6469	F9 V	600	H
980611	90	M71A6	HR7580	B9.5 V	600	2.06
980611	90	HR6018	HR6064	G1 V	600	HK
980611	90	HR2701	HR6064	G1 V	600	HK
980611	90	BCCyg	HR7887	F0 V	600	1.54-2.19
980611	90	BICyg	HR7887	F0 V	600	1.54-2.19
980611	90	KYCyg	HR7887	F0 V	600	1.54-2.19
981002	90	HR6817	HR6847	F7 V	600	HK
981002	90	S089499	HR8250	F7 V	600	HK
981002	90	HR0843	HR0761	F8 V	600	HK
981002	90	HR1939	HR2141	G0 V	600	H,2.06-2.19
981003	90	S050265	HR8170	F7 V	600	2.245-2.42
981003	90	S050296	HR8170	F7 V	600	2.245-2.42
981003	90	S050381	HR8170	F7 V	600	2.245-2.42
981003	90	HR8062	HR8170	F7 V	600	2.24-2.42
981003	90	HR8860	HR8853	F0 V	600	2.25-2.35
981003	90	HR8832	HR8853	F0 V	600	2.25-2.35
981003	90	HR0265	HR0297	F6 V	600	2.19-2.42
981003	90	S011591	HR0297	F6 V	600	2.19-2.42
981003	90	S011620	HR0297	F6 V	600	2.19-2.42
981003	90	S022188	HR0297	F6 V	600	2.19-2.42
981003	90	HR1015	HR0869	F6 V	600	2.24-2.42
981004	90	H339034	HR7386	F7 V	600	1.71
981004	90	M71A9	HR7580	B9.5 V	600	2.06-2.19
981004	90	N188II181	HR0357	F5 V	600	2.06-2.245
981004	90	N188II181	HR9034	F5 V	600	2.31-2.42
981004	90	HR1939	HR2141	G0 V	600	2.24-2.42
981004	90	HR1779	HR2141	G0 V	600	2.37-2.42
981004	90	HR1726	HR2141	G0 V	600	2.37-2.42
981004	90	HR1805	HR2141	G0 V	600	2.37-2.42
981004	90	S77179	HR2141	G0 V	600	2.37-2.42
981005	90	M71A9	HR7580	B9.5 V	600	1.62-1.71,2.24-2.42
981005	90	C468	HR0005	G5 V	600	H
981005	90	C501	HR0005	G5 V	600	H
981005	90	C669	HR0005	G5 V	600	H
981005	90	C971	HR0005	G5 V	600	H
981005	90	HR0265	HR0297	F6 V	600	1.54-1.62
981005	90	S011591	HR0297	F6 V	600	1.54-1.62
981005	90	S011620	HR0297	F6 V	600	1.54-1.62
981005	90	S022188	HR0297	F6 V	600	1.54-1.62
981005	90	HR1015	HR0869	F6 V	600	HK
981005	90	HR1779	HR2141	G0 V	600	2.24-2.31
981005	90	HR1726	HR2141	G0 V	600	2.24-2.31
981005	90	HR1805	HR2141	G0 V	600	2.24-2.31
981005	90	S077179	HR2141	G0 V	600	2.24-2.31

Table 2—*Continued*

Date (1)	Site (2)	Star (3)	Std. (4)	Sp.T. (5)	Gr. (6)	Range (7)
981006	90	M71A9	HR7580	B9.5 V	600	1.54
981006	90	M71A4	HR7580	B9.5 V	600	2.06-2.24
981006	90	S105082	HR7580	B9.5 V	600	1.54-2.24
981006	90	S050265	HR8170	F7 V	600	1.54-2.19
981006	90	S050296	HR8170	F7 V	600	1.54-2.19
981006	90	S050381	HR8170	F7 V	600	1.54-2.19
981006	90	HR8062	HR8170	F7 V	600	1.54-2.19
981006	90	HR0265	HR0297	F6 V	600	2.06-2.13
981006	90	S011591	HR0297	F6 V	600	2.06-2.13
981006	90	S011620	HR0297	F6 V	600	2.06-2.13
981006	90	N188II181	HR9034	F6 V	600	H
981006	90	N188I69	HR9034	F6 V	600	1.54-2.13
981006	90	HR1779	HR2141	G0 V	600	1.70-2.19
981006	90	HR1726	HR2141	G0 V	600	1.70-2.19
981006	90	HR1805	HR2141	G0 V	600	1.70-2.19
981006	90	S077179	HR2141	G0 V	600	1.70-2.19
981007	90	HR7317	HR7454	F5 V	600	H
981007	90	HR7430	HR7454	F5 V	600	H
981007	90	HR7429	HR7560	F8 V	600	H
981007	90	HR7576	HR7451	F7 V	600	H
981007	90	M71A4	HR7580	B9.5 V	600	2.31-2.42
981007	90	N188I69	HR0357	F5 V	600	2.13-2.42
981007	90	HR1779	HR2141	G0 V	600	1.54-1.62
981007	90	HR1726	HR2141	G0 V	600	1.54-1.62
981007	90	HR1805	HR2141	G0 V	600	1.54-1.62
981007	90	S077179	HR2141	G0 V	600	1.54-1.62
990403	90	HR4932	HR5011	G0 V	600	HK
990403	90	HR5366	HR5011	G0 V	600	1.54-2.13
990403	90	HR5480	HR5384	G0 V	600	1.54-2.13
990404	90	HR4932	HR5011	G0 V	600	1.71,2.42
990404	90	HR5366	HR5384	G1 V	600	2.13-2.42
990404	90	HR5480	HR5384	G1 V	600	2.13-2.42
990405	90	HR1907	HR2208	G2 V	600	H
990405	90	HR2600	HR2483	G0 V	600	HK
990405	90	HR2459	HR2483	G0 V	600	HK
990405	90	HR2153	HR2483	G0 V	600	H,2.06
990405	90	HR4267	HR4079	F6 V	600	K
990405	90	M3IV25	HR4983	G0 V	600	HK
990406	90	HR2574	HR2866	F8 V	600	K
990406	90	HR2970	HR2866	F8 V	600	HK
990406	90	HR3845	HR3901	F8 V	600	HK
990406	90	HR4365	HR4437	G0 V	600	H
990406	90	M5IV19	HR5721	F0 V	600	H,2.06,2.13
990406	90	M5IV59	HR5721	F0 V	600	H
990406	90	HR5582	HR5455	F5 V	600	1.70
990406	90	HR5690	HR5583	F8 V	600	HK
990406	90	HR5694	HR5583	F8 V	600	HK
990406	90	HR6815	HR6831	F8 V	600	H
990406	90	HR6872	HR6831	F8 V	600	H
990521	90	M5IV19	HR5721	F0 V	600	2.06-2.31
990521	90	M5IV59	HR5721	F0 V	600	2.06-2.31
990521	90	B133	HR6836	G0 V	600	2.06,2.13
990521	90	BMB285	HR6836	G0 V	600	2.06,2.13

Table 2—*Continued*

Date (1)	Site (2)	Star (3)	Std. (4)	Sp.T. (5)	Gr. (6)	Range (7)
990521	90	BMB179	HR6836	G0 V	600	2.06,2.13
990521	90	BMB142	HR6836	G0 V	600	2.06,2.13
990521	90	BMB087	HR6836	G0 V	600	2.13
990521	90	M92XII8	HR6469	G9 V	600	2.06-2.24
990522	90	HR6815	HR6831	F8 V	600	K
990522	90	HR6872	HR6831	F8 V	600	K
990522	90	M92XII8	HR6469	G9 V	600	2.31-2.42
990522	90	S089499	HR8250	F7 V	600	2.37-2.42
990522	90	HR8165	HR8250	F7 V	600	2.37-2.42
990523	90	M5IV19	HR5721	F0 V	600	2.37-2.42
990523	90	M5IV59	HR5721	F0 V	600	2.37-2.42
990523	90	BMB239	HR6836	G0 V	600	1.60
990523	90	BMB181	HR6836	G0 V	600	1.60
990523	90	BMB289	HR6836	G0 V	600	1.60
990523	90	TLE205	HR6836	G0 V	600	1.60
990523	90	HR7317	HR7454	F7 V	600	K
990523	90	HR7430	HR7454	F7 V	600	K
990523	90	S089499	HR8250	F7 V	600	2.06-2.31
990523	90	HR8165	HR8250	F7 V	600	2.06-2.31
990524	90	HR5854	HR5859	F7 V	600	2.06
990524	90	HR5854	HR5779	F7 V	600	2.13
990524	90	S121191	HR5859	A0 V	600	2.06,2.245-42
990524	90	S121191	HR5779	F7 V	600	2.13,2.19
990524	90	HR5888	HR5859	A0 V	600	2.06,2.245-42
990524	90	HR5888	HR5779	F7 V	600	2.13,2.19
990524	90	HR6136	HR5859	A0 V	600	2.06,2.245-42
990524	90	HR6136	HR5779	F7 V	600	2.13,2.19
990524	90	BMB194	HR6836	G0 V	600	1.60
990524	90	BMB039	HR6836	G0 V	600	1.60
990524	90	HR7148	HR7079	F8 V	600	H
990524	90	HR7171	HR7079	F8 V	600	H
990524	90	S089499	HR8250	F7 V	600	H
990524	90	HR8165	HR8250	F7 V	600	H
990525	90	HR5739	HR5933	F6IV	600	HK
990525	90	HR5744	S029078	F9 V	600	K
990525	90	S121191	HR5859	A0 V	600	H
990525	90	HR5888	HR5859	A0 V	600	1.54-1.62
990525	90	HR6136	HR5859	A0 V	600	H
990525	90	HR6770	HR6976	A1 V	600	1.54-2.13
990525	90	S123779	HR6976	A1 V	600	1.54-2.13
990525	90	HR7176	HR6976	A1 V	600	1.54-2.13
990525	90	HR7429	HR7560	F8 V	600	K
990525	90	HR7576	HR7522	G0 V	600	K
990525	90	S021465	HR0244	F8 V	600	H,2.06
990525	90	HR0265	HR0244	F8 V	600	H,2.06
990526	90	S082685	HR4983	F9.5 V	600	2.06
990526	90	HR6770	HR6976	A1 V	600	2.19-2.42
990526	90	S123779	HR6976	A1 V	600	2.19-2.42
990526	90	HR7176	HR6976	A1 V	600	2.19-2.42
990526	90	HR7759	HR7638	A3 V	600	HK
990526	90	HR7762	HR7638	A3 V	600	HK
990526	90	HR7314	HR7638	A3 V	600	HK
990526	90	HR7735	HR7638	A3 V	600	1.70

TABLE 2—*Continued*

Date (1)	Site (2)	Star (3)	Std. (4)	Sp.T. (5)	Gr. (6)	Range (7)
990526	90	S069578	HR7638	A3 V	600	HK
990526	90	S069825	HR7638	A3 V	600	HK
990526	90	HR8924	HR8931	F8 V	600	HK
990527	90	HR7576	HR7522	G0 V	600	H
990527	90	S105082	HR7560	F8 V	600	HK
990527	90	HR7609	HR7560	F8 V	600	HK
990527	90	HR7847	HR8170	F7 V	600	H
990527	90	HR8665	HR8548	F7 V	600	H
990527	90	HR0163	HR9107	G2 V	600	H
990202	90	N188I105	HR0357	F5 V	600	H,2.17
990202	90	N188II72	HR0357	F5 V	600	H,2.17
990202	90	HR2503	HR2779	G0 V	600	2.25
990202	90	HR3428	HR3510	G1 V	600	1.54
990202	90	H77729	HR3563	F6 V	600	HK
990203	90	HR0617	HR0869	F6 V	600	K
990203	90	HR0843	HR0869	F6 V	600	HK
990203	90	HR0867	HR0869	F6 V	600	K
990203	90	HR1015	HR0869	F6 V	600	HK
990203	90	HR3369	HR3299	F6 V	600	2.24-2.42
990203	90	HR3427	HR3299	F6 V	600	2.24-2.42
990203	90	HR3428	HR3299	F6 V	600	2.24-2.42
990203	90	HR3461	HR3299	F6 V	600	2.31-2.42

NOTE.—Columns: (1) Date of the observation, in yymmdd format, e.g. 990203 is the night of Feb 3-4, 1999; (2) Sites: 61, 90, MM - Steward Observatory 1.55-m, 2.3-m, and the original MMT telescopes, respectively; (3) Object, S=SAO, H=HD, N=NGC, B=BD; (4) Standard star for the atmospheric correction; (5) Spectral Type for the standard star; (6) Gratings: 600 lines mm^{-1} corresponds to spectral resolution R≈3000, and 300 lines mm^{-1} corresponds to R≈1500; (7) Spectral range covered: H and K indicate that the entire atmospheric window was observed. Numbers give the central wavelength of the observed grating settings in μm. Two numbers separated by a dash means that all grating settings in between them were observed. A number in brackets after H and/or K with a minus indicates a missing setting.

Table 3

Adopted photospheric parameters of the stars. The complete table is presented in the electronic edition only.

Stellar ID[a]					Sp.	Photospheric Parameters[b]			
HR	HD	SAO	BD	Other	Class	T_{eff}	$\log g$	[Fe/H]	Method[c]
(1)	(2)	(3)	(4)	(5)	(6)	(7)	(8)	(9)	(10)
					SUPERGIANTS				
	104452	82106	22 2430	1Com	G0 II(32)	-1	99.99	0.00(1)	-
7063	173764	142618	-4 4582	βSct	G4 IIa(32)	4700(2)	0.94(2)	-0.15(2)	s
7314	180809	68065	37 3398	θLyr	K0 II(32)	4550(2)	1.77(2)	0.14(2)	s
6713	164349	103285	16 3335	93Her	K0.5 II(32)	4383(2)	1.80(2)	-0.22(2)	s
	193515	69825	37 3882	PPM84702	K1 II(33)	-1	99.99	0.00(1)	-
8465	210745	34137	57 2475	ζCep	K1.5 Ib(32)	4159(2)	0.88(2)	0.25(2)	s
7735	192577	32042	52 2547	o01Cyg	K2 Ib(34)	4030(5)	1.39(5)	-0.36(5)	s
	192041	69578	38 3939	PPM84402	K2 II(33)	-1	99.99	0.00(1)	-
6498	157999	122387	4 3422	σOph	K2 II(32)	-1	99.99	0.01(30)	s
	232078	105082	16 3924	V339Sge	K3 II(35)	4000(7)	0.40(7)	-1.60(7)	s
6418	156283	65890	36 2844	πHer	K3 II(32)	4100(2)	1.68(2)	-0.18(2)	s
7475	185622A	105104	16 3936	GC27195	K4 Ib(32)	4000(13)	0.70(13)	-0.12(13)	s
7762	193217	49425	42 3670	GC28214	K4 II(27)	4000(67)	0.80(67)	0.06(21)	s
2289	44537	41076	49 1488	ψ01Aur	K5-M0 Iab-Ib(32)	3055(30)	99.99	0.08(30)	s
	163428	185981		GC24397	K5 II(36)	3800(13)	0.60(13)	-0.14(13)	s
5594	132933	120798	0 3297	GC20212	M0.5 IIb(32)	-1	99.99	0.00(1)	-
4666	106609	44097	41 2284	2CVn	M0.5 III(32)	-1	99.99	0.00(1)	-
	236697	22188	57 258	V466Cas	M0.5 Ib(32)	3500(12)	99.99	0.00(1)	-
	339034		24 3902	NRVul	M1 Ia(32)	-1	99.99	0.00(1)	-
	35601	77179	29 897	V362Aur	M1.5 Iab-Ib(32)	4000(2)	0.70(2)	-0.24(2)	s
1939	37536	58322	31 1049	ϕAur	M2 Iab(37)	3789(2)	0.70(2)	-0.15(2)	s
	239978	34529	56 2793	STCep	M2 Ia-Iab(32)	-1	99.99	0.00(1)	-
	202380	33232	59 2342	V419Cep	M2 Ib(32)	3600(13)	0.60(13)	0.07(29)	s
4362	97778	81736	23 2322	72Leo	M3 IIb(32)	3300(28)	99.99	0.00(1)	-
		50296	45 3349	AZCyg	M3 Iab(32)	3200(12)	99.99	0.00(1)	-
				KYCyg	M3.5 Ia(38)	3100(11)	99.99	0.00(1)	-
			37 3903	BCCyg	M3.5 Ia(38)	3673(4)	99.99	0.00(1)	-
		11591	62 207	HSCas	M4 Ia(37)	-1	99.99	0.00(1)	-
			36 4025	BICyg	M4 Iab(38)	3673(4)	99.99	0.00(1)	-
7139	175588	67559	36 3319	δ02Lyr	M4 II(32)	3637(4)	99.99	0.00(1)	-
7009	172380	67193	39 3476	XYLyr	M4.5-M5+ II(32)	3351(4)	99.99	0.00(1)	-
					GIANTS				
				NGC7789K676	III	4988(3)	2.51(3)	-0.10(3)	s; $(V-K)_0$=2.12(3)
				NGC7789K875	III	4965(3)	2.39(3)	-0.10(3)	s; $(V-K)_0$=2.16(3)
				NGC7789K897	III	4965(3)	2.45(3)	-0.10(3)	s; $(V-K)_0$=2.16(3)
			36 4025	M67F84	III	4763(3)	2.30(3)	-0.10(3)	s; $(V-K)_0$=2.32(3)
				NGC7789K859	III	4626(3)	2.18(3)	-0.10(3)	s; $(V-K)_0$=2.46(3)
				NGC7789K575	III	4512(3)	2.00(3)	-0.10(3)	s; $(V-K)_0$=2.60(3)
				NGC188I105	III	4585(3)	2.29(3)	0.00(3)	s; $(V-K)_0$=2.51(3)
				M92XII8	III	4488(3)	1.93(3)	-2.20(3)	s; $(V-K)_0$=2.63(3)
				NGC188I69	III	4401(3)	2.36(3)	0.00(3)	s; $(V-K)_0$=2.75(3)
				NGC188II72	III	4387(3)	1.93(3)	0.00(3)	s; $(V-K)_0$=2.77(3)
				M03IV25	III	4355(3)	1.04(3)	-1.70(3)	s; $(V-K)_0$=2.82(3)
				NGC188II181	III	4276(3)	1.35(3)	0.00(3)	s; $(V-K)_0$=2.95(3)
				M05IV59	III	4300(3)	1.46(3)	-1.30(3)	s; $(V-K)_0$=2.91(3)
				NGC7789K468	III	4228(3)	1.72(3)	-0.10(3)	s; $(V-K)_0$=3.03(3)

Table 3—*Continued*

		Stellar ID[a]			Sp.		Photospheric Parameters[b]		
HR	HD	SAO	BD	Other	Class	T_{eff}	$\log g$	[Fe/H]	Method[c]
(1)	(2)	(3)	(4)	(5)	(6)	(7)	(8)	(9)	(10)
				M03III28	III	4122(3)	0.86(3)	-1.70(3)	s; $(V\text{-}K)_0$=3.21(3)
				M05III3	III	4095(3)	1.50(3)	-1.30(3)	s; $(V\text{-}K)_0$=3.26(3)
				NGC7789K501	III	4085(3)	1.58(3)	-0.10(3)	s; $(V\text{-}K)_0$=3.28(3)
				M71A4	III	4028(3)	1.90(3)	-0.56(3)	s; $(V\text{-}K)_0$=3.40(3)
				M71A6	III	-1	99.99	-0.56(3)	s; $(V\text{-}K)_0$=3.55(3)
				M13B786	III	3963(3)	0.62(3)	-1.50(3)	s; $(V\text{-}K)_0$=3.57(3)
				NGC7789K971	III	3831(3)	0.89(3)	-0.10(3)	s; $(V\text{-}K)_0$=3.96(3)
				NGC7789K415	III	3859(3)	0.78(3)	-0.10(3)	s; $(V\text{-}K)_0$=3.88(3)
				NGC188s359	III	-1	99.99	0.00(3)	s; $(V\text{-}K)_0$=2.12(3)
				NGC188s473	III	-1	99.99	0.00(3)	s; $(V\text{-}K)_0$=2.12(3)
				TLE205	III(31)	-1	99.99	-0.21(1)	-
7171	176301	104272	17 3779	GC25999	B7 III-IV(39)	13100(7)	3.50(7)	0.00(7)	s
5694	136202	120946	2 2944	5Ser	F8 IV(40)	6030(7)	3.89(7)	-0.07(7)	s
4883	111812	82537	28 2156	31Com	G0 IIIp(32)	-1	99.99	99.99	-
163	3546	74164	28 103	ϵAnd	G6 III(32)	4957(3)	2.60(3)	-0.81(3)	s
4716	107950	28366	52 1626	5CVn	G6 III(32)	5347(2)	2.31(2)	-0.25(2)	s
5480	129312	120601	8 2903	31Boo	G7 IIIa(32)	4834(3)	1.55(3)	-0.08(3)	s
4418	99648	118875	3 2504	τLeo	G7.5 IIIa(32)	4850(2)	1.90(2)	0.36(2)	s
265	5395	21855	58 138	υCas	G8 IIIb(32)	4819(3)	2.40(3)	-0.62(3)	s
5681	135722	64589	33 2564	δBoo	G8 III(32)	4834(3)	2.45(3)	-0.39(3)	s
5888	141680	121215	2 3007	ωSer	G8 III(41)	4707(3)	1.95(3)	-0.29(3)	s
6770	165760	123140	8 3582	71Oph	G8 III(32)	4957(3)	2.00(3)	-0.01(3)	s
4932	113226	100384	11 2529	ϵVir	G8 IIIab(32)	4994(3)	2.10(3)	0.12(3)	s
3427	73665	80333	20 2158	39Cnc	G8 III(32)	4965(3)	2.35(3)	0.24(3)	s
4400	99055	118831	2 2418	79Leo	G8 III(32)	-1	99.99	0.29(5)	n
7430	184492	162792	-10 5122	37Aql	G8.5 IIIa(32)	4536(3)	1.50(3)	-0.12(3)	s
2153	41636	40881	41 1365	GC7780	G9 III(42)	4690(7)	2.50(7)	-0.16(7)	s
5366	126454	139866	-1 2938	υVir	G9 III(32)	4755(7)	2.50(7)	-0.10(7)	s
2970	61985	134986	-9 2172	αMon	G9 III(32)	4776(3)	2.20(3)	-0.03(3)	s
3369	72324	80245	24 1946	υ02Cnc	G9 III(43)	4864(3)	1.60(3)	-0.02(3)	s
3428	73710	98021	20 2166	GC11899	G9 III(32)	4864(3)	2.10(3)	0.16(3)	s
	141144	121191	1 3131	GC21220	K0 III(44)	-1	99.99	99.99	-
	172401	123779	8 3791	PPM166313	K0 III(45)	-1	99.99	99.99	-
	114401	82685	29 2374	UBV11896	K0 III(46)	-1	99.99	99.99	-
1907	37160	112958	9 898	ϕ02Ori	K0 IIIb(32)	4751(3)	2.90(3)	-0.70(3)	s
2701	54810	134282	-4 1840	20Mon	K0 III-IV(42)	4697(3)	2.35(3)	-0.25(3)	s
4287	95272	156375	-17 3273	αCrt	K0+ III(32)	4635(3)	2.15(3)	0.05(3)	s
3461	74442	98087	18 2027	δCnc	K0 III(32)	4651(3)	2.10(3)	0.16(3)	s
3994	88284	155785	-11 2820	λHya	K0 III(32)	4971(3)	2.70(3)	0.39(3)	s
4668	106760	62928	33 2213	GC16754	K0.5 IIIb(32)	4510(2)	2.70(2)	-0.29(2)	s
5196	120452	158186	-17 3937	89Vir	K0.5 III(32)	4760(7)	2.60(7)	0.03(7)	s
8165	203344	89640	23 4294	34Vul	K1 III(42)	4669(3)	2.60(3)	-0.24(3)	s
6018	145328	65108	36 2699	τCrB	K1- III(32)	4678(3)	2.50(3)	-0.14(3)	s
6817	167042	30784	54 1950	GC24820	K1 III(48)	4949(3)	3.05(3)	-0.11(3)	s
8841	219449	146598	-9 6156	ψ01Aqr	K1- III(32)	4635(3)	2.55(3)	-0.04(3)	s
7148	175743	104272	17 3779	GC25999	K1 III(49)	4635(3)	2.45(3)	0.02(3)	s
7176	176411	104318	14 3736	ϵAql	K1- III(32)	4687(3)	2.10(3)	0.08(3)	s
3418	73471	116988	3 2026	σHya	K1 III(32)	4480(3)	1.70(3)	0.24(3)	s
1779	35295	57999	34 1031	GC6650	K1 III-IV(47)	-1	2.80(6)	0.29(5)	s
3360	72184	60890	38 1920	GC11684	K1.5 IIIb(32)	4669(3)	2.65(3)	0.33(3)	s
	201626	89499	26 4091	UBV18320	K2 III(50)	4941(30)	99.99	-1.45(8)	s
2600	51440	59658	38 1656	62Aur	K2 III(48)	4381(3)	2.20(3)	-0.52(3)	s

Table 3—*Continued*

HR	HD	SAO	BD	Other	Sp. Class	T_{eff}	$\log g$	[Fe/H]	Method[c]
	Stellar ID[a]					Photospheric Parameters[b]			
(1)	(2)	(3)	(4)	(5)	(6)	(7)	(8)	(9)	(10)
5616	133582	83645	27 2447	43Boo	K2 III(32)	4280(2)	2.30(2)	-0.35(2)	s
5947	143107	84098	27 2558	ϵCrB	K2 IIIab(32)	4318(3)	1.70(3)	-0.34(3)	s
617	12929	75151	22 306	αAri	K2- IIIab(32)	4480(3)	2.10(3)	-0.22(3)	s
6872	168775	66869	36 3094	κLyr	K2- IIIab(32)	4520(3)	1.70(3)	0.04(3)	s
5744	137759	29520	59 1654	ιDra	K2 III(32)	4504(3)	2.05(3)	0.08(3)	s
2697	54719	59858	30 1439	τGem	K2 III(32)	4381(3)	1.35(3)	0.18(3)	s
5854	140573	121157	6 3088	αSer	K2 IIIb(32)	4528(3)	2.10(3)	0.23(3)	s
3905	85503	81064	26 2019	μLeo	K2 III(32)	4480(3)	2.15(3)	0.41(3)	s
1726	34334	57853	33 1000	16Ari	K2.5 III(32)	4234(3)	2.15(3)	-0.30(3)	s
3845	83618	137035	0 2231	ιHya	K2.5 III(32)	4240(3)	1.15(3)	-0.03(3)	s
4521	102328	28142	56 1544	GC16153	K2.5 IIIb(32)	4457(3)	2.35(3)	0.46(3)	s
5582	132345	120601	8 2903	GC20157	K3- III(32)	4374(3)	1.60(3)	0.48(3)	s
2854	58972	115478	9 1660	γCMi	K3 III(32)	4023(8)	2.00(8)	-0.30(8)	s
6364	154733	84835	22 3073	GC23089	K3 III(32)	4220(2)	2.20(2)	-0.14(2)	s
4365	97907	99525	14 2367	nLeo	K3 III(41)	4351(8)	2.07(8)	-0.04(8)	s
1015	20893	75899	20 551	τAri	K3 III(41)	4355(3)	1.95(3)	0.07(3)	s
7429	184406	124799	7 4132	μAql	K3- IIIb(32)	4428(3)	2.45(3)	0.08(3)	s
7759	193092	49410	39 4114	GC28197	K3 IIIa(32)	4065(20)	99.99	0.12(5)	n
5370	125560	100908	16 2637	20Boo	K3 III(41)	4381(3)	1.65(3)	0.22(3)	s
7576	188056	32042	52 2547	20Cyg	K3 III(32)	4355(3)	2.15(3)	0.43(3)	s
8924	221148	146736	-5 5999	34Vul	K3- IIIb(32)	4643(3)	3.05(3)	0.50(3)	s
1805	35620	58051	34 1048	ϕAur	K3.5 III(32)	4156(3)	1.20(3)	0.22(3)	s
7317	180928	162462	-15 5310	GC26626	K4 III(36)	3969(3)	1.30(3)	-0.49(3)	s
	77729	80616	26 1895	HIP44592	K4 III(48)	4271(2)	2.00(2)	-0.40(2)	s
2574	50778	152071	-11 1681	θCMa	K4 III(41)	4019(3)	1.35(3)	-0.20(3)	s
3249	69267	116569	9 1917	βCnc	K4 III(32)	4032(3)	1.60(3)	-0.12(3)	s
5600	133124	83624	25 2861	41Boo	K4 III(32)	3960(2)	1.68(2)	-0.04(2)	s
2503	49161	114410	8 1496	17Mon	K4 III(41)	4276(3)	1.85(3)	0.13(3)	s
6136	148513	121623	0 3529	GC22148	K4 III(41)	4046(3)	1.00(3)	0.25(3)	s
224	4656	109474	6 107	δPsc	K4.5 IIIb(32)	3953(3)	1.10(3)	-0.08(3)	s
4954	113996	82659	28 2185	41Com	K5- III(32)	3970(2)	1.69(2)	-0.26(2)	s
5826	139669	8274	77 592	θUMi	K5- III(32)	3915(3)	1.00(3)	-0.02(3)	s
2459	47914	41288	44 1518	ψ04Aur	K5 III(41)	3999(3)	1.40(3)	0.09(3)	s
5690	136028	140444	0 3337	GC20750	K5 III(51)	4040(8)	1.90(8)	0.14(8)	s
843	17709	55946	34 527	17Per	K5.5 III(32)	3905(8)	1.10(8)	-0.18(8)	s
4986	114780	100460	12 2565	GC17884	M0 III(52)	-1	99.99	99.99	-
4299	95578	137947	-1 2471	61Leo	M0 III(32)	3700(2)	1.40(2)	-0.23(2)	s
4069	89758	43310	42 2115	μUMa	M0 III(32)	-1	99.99	0.00(15)	s
8795	218329	127976	8 4997	55Peg	M1 IIIab(32)	3810(7)	1.10(7)	99.99	-
5739	137471	101545	15 2585	τ01Ser	M1 III(48)	3810(7)	1.10(7)	0.00(7)	s
5800	139153	64790	39 2889	μCrB	M1.5 IIIb(32)	-1	99.99	99.99	-
8860	219734	52871	48 3991	8And	M2.5 III(32)	3730(7)	0.90(7)	99.99	-
5932	142780	45788	43 2542	2Her	M3- III(32)	3756(19)	99.99	99.99	-
6815	167006	66737	31 1536	104Her	M3 III(32)	3640(7)	0.70(7)	0.00(7)	s
4184	92620	62206	32 2066	RXLMi	M3.5 III(32)	-1	99.99	0.00(15)	s
				B133	M4 III(66)	-1	99.99	-0.21(1)	-
6242	151732	46288	42 2749	GC22611	M4.5 III(32)	-1	99.99	99.99	-
8062	200527	50381	44 3679	V1981Cyg	M4.5 III(32)	3451(2)	0.70(2)	-0.04(2)	s
4909	112264	44383	47 2003	TUCVn	M5- III(32)	3350(4)	99.99	99.99	-
4267	94705	118576	6 2369	VYLeo	M5.5 III(32)	3335(7)	0.20(7)	99.99	-
867	18191	93189	17 457	ρ02Ari	M6- III(32)	3250(7)	0.30(7)	99.99	-
6146	148783	46108	42 2714	GHer	M6- III(32)	3250(7)	0.20(7)	-0.06(7)	s

Table 3—*Continued*

		Stellar ID[a]			Sp.	Photospheric Parameters[b]			
HR (1)	HD (2)	SAO (3)	BD (4)	Other (5)	Class (6)	$T_{\rm eff}$ (7)	$\log g$ (8)	[Fe/H] (9)	Method[c] (10)
				BMB194,V1460 Sgr	M6.5 III(65)	-1	99.99	-0.21(1)	-
				BMB239	M6.5 III(65)	-1	99.99	-0.21(1)	-
				BMB179	M7 III(65)	-1	99.99	-0.21(1)	-
				BMB181	M7 III(65)	-1	99.99	-0.21(1)	-
				BMB285	M7 III(65)	-1	99.99	-0.21(1)	-
				BMB087	M8 III(65)	-1	99.99	-0.21(1)	-
				BMB142	M8 III(65)	-1	99.99	-0.21(1)	-
				BMB039	M9 III(65)	-1	99.99	-0.21(1)	-
				BMB289	M9 III(65)	-1	99.99	-0.21(1)	-
				DWARFS					
3314	71155	135896	-3 2339	30Mon	A0 V(53)	9806(9)	99.99	99.99	-
5144	119055	82942	20 2858	1Boo	A0 IV(55)	9485(28)	99.99	99.99	-
3481	74873	98117	12 1904	δCnc	A1 V(54)	-1	99.99	99.99	-
4380	98353	62491	38 2225	55UMa	A2 V(54)	9120(28)	99.99	99.99	-
7451	184960	31782	50 1326	GC27068	F7 V(56)	6272(2)	4.37(2)	-0.16(2)	s
5270	122563	120251	10 2617	GC18965	G0 IV(48)	4626(3)	1.50(3)	-2.67(3)	s
4785	109358	44230	42 2321	βCVn	G0 V(53)	5903(2)	4.42(2)	-0.12(2)	s
6212	150680	65485	31 2884	ζHerA	G0 IV(32)	5740(2)	3.70(2)	-0.07(2)	s
5235	121370	100766	19 2725	ηBoo	G0 IV(32)	6036(7)	3.72(7)	0.38(7)	s
5829	139777	2556	80 480	GC20929	G2 V(58)	-1	99.99	-0.25(57)	n
5409	126868	139951	-1 2957	ϕVir	G2 IV(32)	5640(17)	3.80(17)	-0.07(5)	n
3538	76151	136389	-4 2490	GC12307	G2 V(32)	5715(2)	4.41(2)	0.03(2)	s
5853	140538	121152	2 2989	ψSer	G2.5 V(32)	-1	99.99	0.01(18)	n
5072	117176	100582	14 2621	70Vir	G4 V(32)	5530(10)	4.05(10)	-0.05(10)	s
6623	161797	85397	27 2888	μHer	G5 IV(32)	5390(7)	3.83(7)	0.23(7)	s
5019	115617	157844	-17 3813	61Vir	G6.5 V(32)	5600(2)	4.24(2)	0.22(3)	s
3259	69830	154093	-12 2449	GC11325	G7.5 V(32)	5485(14)	4.50(14)	-0.03(14)	s
	6009	74439	24 163	GC1231	G8 IV(59)	-1	99.99	99.99	-
4496	101501	62655	35 2270	61UMA	G8 V(32)	5360(3)	4.35(3)	-0.39(3)	s
	7010	11620	59 199	UBV1226	K0 IV(60)	-1	99.99	-0.28(8)	s
7957	198149	19019	61 2050	ηCep	K0 IV(32)	4971(3)	3.20(3)	-0.26(3)	s
6752	165341	123107	2 3482	70Oph	K0- V(32)	5260(2)	5.00(2)	-0.25(2)	s
166	3651	74175	20 85	54Psc	K0 V(32)	5487(3)	4.50(3)	0.17(3)	s
	145675	45933	44 2594	14Her	K0 V(32)	5353(3)	4.55(3)	0.27(3)	s
1325	26965	131063	-7 780	o02Eri	K0.5 V(32)	5050(3)	4.66(3)	-0.17(3)	s
5553	131511	101276	19 2881	DEBoo	K0.5 V(32)	-1	99.99	-0.13(18)	n
5901	142091	64948	36 2652	κCrB	K1 IVa(32)	4751(3)	2.85(3)	0.00(3)	s
493	10476	74883	19 279	107Psc	K1 V(32)	5065(3)	4.55(3)	-0.10(3)	s
	199580	50265	42 3915	GC29247	K1 IV(48)	5039(3)	3.50(3)	-0.05(3)	s
6014	145148	121392	6 3169	G16-32	K1.5 IV(32)	4849(3)	3.45(3)	0.10(3)	s
222	4628	109471	4 123	V339Sge	K2 V(61)	4960(3)	4.35(3)	-0.32(3)	s
	109011	28414	55 1536	GJ1160	K2 V(32)	-1	99.99	-0.28(23)	b
	184467	28414	58 1929	GJ762.1	K2 V(32)	-1	99.99	-0.20(18)	n
	160346	122610	3 3465	GJ688	K3- V(32)	-1	99.99	-0.15(18)	n
8832	219134	35236	56 2966	GC32329	K3 V(32)	4824(3)	4.41(3)	-0.04(3)	s
5568	131977	183040	-20 4125	GJ570A	K4 V(32)	4624(3)	4.70(3)	0.10(3)	s
8085	201091	70919	38 4343	61CygA	K5 V(32)	4450(2)	4.68(2)	-0.37(2)	s
	88230	43223	50 1725	GJ380,LHS280	K6e V(32)	3917(3)	4.68(3)	0.28(3)	s
8086	201092		38 4343	61CygB	K7 V(32)	4120(2)	4.40(2)	-0.63(2)	s
	157881	122374	2 3312	GJ673,LHS447	K7 V(56)	4180(2)	4.70(2)	-0.20(2)	s
	79211	27179	53 1321	GJ338B	M0 V(48)	3769(7)	4.71(7)	0.06(22)	b

Table 3—*Continued*

			Stellar ID[a]		Sp.		Photospheric Parameters[b]		
HR	HD	SAO	BD	Other	Class	T_{eff}	$\log g$	[Fe/H]	Method[c]
(1)	(2)	(3)	(4)	(5)	(6)	(7)	(8)	(9)	(10)
				GJ625,HIP80459	M1.5 V(62)	-1	99.99	99.99	-
	131976	183039	-20 4123	GJ570B	M1.5 V(32)	3506(3)	4.73(3)	0.00(3)	s
	1326A	36248	43 44A	GJ15A(SW)	M2 V(32)	3721(16)	5.00(16)	-1.50(16)	b
	95735	62377	36 2147	GJ411,LHS37	M2 V(32)	3620(2)	4.90(2)	-0.20(2)	s
		43609	44 2051	GJ412A,LHS38	M2 V(48)	3544(3)	4.85(3)	-0.19(22)	b
	119850	100695	15 2620	GJ526,LHS47	M2 V(32)	3300(28)	99.99	0.05(22)	b
		81292	20 2465	GJ388,ADLeo	M3 V(62)	3400(25)	4.85(25)	0.00(25)	s
	173739	31128	59 1915	GJ725A,LHS58	M3 V(64)	3450(24)	99.99	0.08(22)	b
	1326B		43 44B	GJ15B(NE),LHS4	M3.5 V(62)	3107(3)	5.08(3)	-0.50(26)	s
				GJ402,LHS294	M4 V(64)	-1	99.99	99.99	-
				GJ213,LHS31	M4 V(64)	3250(25)	5.00(25)	0.00(25)	s
				GJ206,HIP25953	M4e V(63)	3400(25)	4.85(25)	0.10(25)	s
				GJ831,LHS511	M4.5 V(62)	-1	99.99	99.99	-
				GJ866A,LHS68	M5 V(64)	2747(3)	5.09(3)	99.99	s
				GJ65A,LHS9	M5.5 V(64)	3025(28)	5.15(25)	0.00(25)	s
				GJ905,LHS549	M5.5 V(62)	2799(3)	5.12(3)	0.00(26)	s

Note.—The complete table is presented in the electronic edition. Columns: (1-5) Stellar identifiers: HR, HD, SAO, BD, etc. Abreviations: B = Blanco (1986), BMB = Blanco et al. (1984), and TLE = Lloyd Evans (1976). For more details see Worthey et al. (1994); (6) Spectral classification. The number in brackets is the reference source; (7-9) Photosperic parameters: effective temperature $T_{\rm efff}$, surface gravity $\log g$, abundance [Fe/H]. Unknown entries have values -1 for $T_{\rm efff}$, and 99.99 for $\log g$ and [Fe/H]. The number in brackets is the reference source; (10) Metod used to estimate the abundance: s - spectroscopy; b - broad band photometry; n - narrow band photometry; "-" - none, the value is unknown or assumed.

References.—(1) tentatively assumed Solar abundance for the supergiants and [Fe/H]=-0.21 for the bulge giants (Ramírez et al. 2000b); (2) Cayrel de Strobel et al. (2000) and references therein; (3) Gorgas et al. (1993) and references therein; (4) van Dyck, Belle & Thompson (1998); (5) Taylor (1999) and references therein; (6) Zhou Xu (1991); (7) Worthey et al. (1994) and references therein; (8) Faber et al. (1985) and references therein; (9) Di Benedetto (1998); (10) Santos et al. (2003); (11) Garmany & Stencel (1992); (12) Lee (1970); (13) Luck & Bond (1989); (14) Feltzing & Gustafsson (1998); (15) Taylor, Spinrad & Schweizer (1972); (16) Alonso, Arribas & Martinez-Roger (1994); (17) Bell & Gustafsson (1989); (18) Eggen (1998); (19) Dumm & Schild (1998); (20) van Belle et al. (1999); (21) Taylor (1991); (22) Eggen (1996); (23) Zakhozhaj & Shaparenko (1996); (24) Kirkpatrick et al. (1993); (25) Leggett et al. (1996); (26) Leggett et al. (2000); (27) Bidelman (1957); (28) Johnson (1966); (29) (Ramírez et al. 2000a); (30) Cayrel de Strobel et al. (1997) and references therein; (31) Lloyd Evans (1976); (32) Keenan & McNeil (1989); (33) Barbier (1962); (34) Ginestet & Carquillat (2002); (35) Preston & Bidelman (1956); (36) Houk & Smith-Moore (1988); (37) Humphreys (1970); (38) Sloan & Price (1998); (39) Cowley (1972); (40) Gray et al. (2001); (41) Roman (1952); (42) Keenan & Keller (1953); (43) Greenstein & Keenan (1958); (44) Upgren & Staron (1970); (45) Fernie (1959); (46) Fehrenbach et al. (1962); (47) Schmidtt (1971); (48) Roman (1955); (49) Halliday (1955); (50) Eaton (1995); (51) Eggen & Stokes (1970); (52) Appenzeller (1967); (53) Johnson & Morgan (1953); (54) Cowley et al. (1969); (55) Lutz & Lutz (1977); (56) Morgan et al. (1953); (57) Haywood (2001); (58) Abt (1981); (59) Harlan (1969); (60) Barbier (1968); (61) Nassau & van Algabada (1947); (62) Henry et al. (1994); (63) Joy & Abt (1974); (64) Kirkpatrick et al. (1997); (65) Blanco et al. (1984); (66) Blanco (1986); (67) Brown et al. (1989)

Table 4
Definitions of spectral bands.

No.	Species	Line[a]		Cont. 1[a]		Cont. 2[a]		Ref.
		$\lambda_c, \AA$	$\Delta\lambda, \AA$	$\lambda_c, \AA$	$\Delta\lambda, \AA$	$\lambda_c, \AA$	$\Delta\lambda, \AA$	
1	MgI (1.50μm)	15040	40	15005	30	15075	30	1
2	FeI (1.58μm)	15830	40	15800	20	15857.5	15	1
3	SiI (1.59μm)	15890	40	15850	40	15930	40	3
4	CO (1.62μm)	16197.5	45	16160	30	16270	30	3
5	MgI (1.71μm)	17115	30	17092.5	15	17145	30	1
6	MgI (2.11μm)	21075	70	21020	40	21130	40	1
7	Brγ (2.16μm)	21662.5	47	20929	44	22899	52	2
8	NaI (2.21μm)	22075	70	22170	60	22350	40	4
9	NaI (2.21μm)	22077	48	20929	44	22899	52	2
10	CaI (2.26μm)	22635	110	22510	40	22720	40	4
11	CaI (2.26μm)	22636.5	51	20929	44	22899	52	2
12	MgI (2.28μm)	22806	52	22750	60	22857	50	1
13	MgI (2.28μm)	22820	60	22720	40	22886	30	4
14	CO (2.29μm)	22950.5	53	22899	52			3
15	^{12}CO$(2,0)$(2.29μm)	22957	52	22899	52			2
16	CO (2.29μm)	22980	100	22850	100			6
17	^{12}CO$(3,1)$(2.32μm)	23245	54	22899	52			2
18	^{13}CO$(2,0)$(2.35μm)	23463.5	55	22899	52			2
19	CO (2.35μm)	23550	900					5

[a]Central wavelength λ_c and band width $\Delta\lambda$, in Å.

References.—(1) This work; (2) Kleinmann & Hall (1986); (3) Origlia, Moorwood & Oliva (1993); (4) Ali et al. (1995); (5) Doyon, Joseph & Wright (1994); (6) Ivanov et al. (2000).

Table 5

Spectral indices of features of interest.

Star ID	Mg	Fe	Si	CO	Mg	Mg	Brγ_k	Na	Na	Ca	Ca	Mg	Mg	CO	CO	CO	CO	CO	CO
									SUPERGIANTS										
SAO082106	0.04	0.01	0.04	0.01	0.00	0.00	0.08	0.01	0.01	0.01	0.00	0.01	0.02	0.02	0.02	0.01	0.01	0.01	0.01
HR7063	0.06	0.04	0.07	0.03	0.02	0.01	0.07	0.00	0.03	0.01	0.03	0.01	0.01	0.16	0.15	0.09	0.14	0.01	0.05
HR7314	0.08	0.03	0.03	0.06	0.03	0.02	0.01	0.03	0.03	0.04	0.05	0.00	0.01	0.06	0.10	0.11	0.20	0.02	0.07
HR6713	0.07	0.03	0.10	0.05	0.03	0.02	0.04	0.00	0.04	0.01	0.02	0.02	0.02	0.22	0.23	0.14	0.19	0.01	0.06
SAO069825	0.07	0.02	0.02	0.02	0.03	0.02	0.07	0.02	0.02	0.02	0.02	0.01	0.01	0.03	0.05	0.06	0.12	0.00	0.04
HR8465	0.10	0.04	0.10	0.11	0.03	0.01	0.03	0.03	0.06	0.01	0.04	0.02	0.01	0.36	0.38	0.25	0.31	0.07	0.09
HR7735					0.04														
SAO069578	0.11	0.03	0.04	0.07	0.04	0.01	0.03	0.04	0.06	0.03	0.05	0.01	0.01	0.06	0.10	0.12	0.24	0.06	0.08
HR6498	0.10	0.02	0.08	0.11	0.03	-0.01	0.00	0.03	0.03	0.00	0.02	0.00	-0.01	0.34	0.34	0.26	0.20	0.02	0.08
SAO105082	0.02	-0.01	0.07	0.04	-0.06	0.01	-0.04	0.00	-0.07	0.00	-0.11	0.00	-0.01	0.03	0.01	0.09	-0.02	-0.09	0.05
HR6418	0.09	0.03	0.10	0.06	0.04	0.01	0.02	0.05	0.06	0.01	0.02	0.01	0.01	0.25	0.24	0.15	0.22	0.04	0.06
HR7475	0.11	0.05	0.07	0.11	0.05	0.02	0.02	0.05	0.08	0.05	0.10	0.02	0.00	0.40	0.38	0.22	0.40	0.07	0.11
HR7762	0.10	0.04	0.05	0.09	0.04	0.01	0.02	0.05	0.06	0.03	0.05	0.01	0.01	0.09	0.14	0.17	0.26	0.06	0.09
HR2289	0.15	0.07	0.11	0.15	0.07	-0.00	0.03	0.08	0.09	0.00	0.02	0.02	0.01	0.20	0.22	0.13	0.45	0.12	0.17
SAO185981	0.15	0.06	0.11	0.15	0.08	0.02	0.01	0.08	0.10	0.05	0.11	0.04	0.04	0.44	0.48	0.29	0.45	0.12	0.14
HR5594	0.06	0.03	0.08	0.08	0.04	0.01	0.02	0.05	0.05	0.03	0.05	0.00	0.00	0.30	0.32	0.21	0.28	0.16	0.09
HR4666	0.09	0.04	0.04	0.07	0.06	0.02	0.01	0.03	0.06	0.03	0.07	0.01	0.01	0.29	0.32	0.20	0.27	0.08	0.07
SAO022188	0.17	0.06	0.09	0.17		0.02	-0.01	0.07	0.09	0.04	0.08	0.03	0.02	0.47	0.50	0.32	0.43	0.10	0.13
HD339034	0.14	0.09	0.11	0.10	0.06	0.01	0.01	0.08	0.10	0.02	0.06	0.03	0.02	0.42	0.45	0.32	0.46	0.08	0.13
SAO077179	0.14	0.07	0.11	0.15	0.06	0.01	-0.00	0.07	0.09	0.04	0.08	0.03	0.01	0.42	0.45	0.27	0.39	0.13	0.12
HR1939	0.13	0.04	0.11	0.16	0.06	0.02	-0.00	0.10	0.11	0.04	0.07	0.03	0.01	0.46	0.50	0.34	0.50	0.13	0.18
SAO034529	0.10	0.03	0.10	0.19	0.02	0.01	0.00	0.07	0.09	0.05	0.08	0.03	0.00	0.53	0.52	0.38	0.42	0.06	0.10
SAO033232	0.10	0.06	0.06	0.15	0.06	0.02	0.03	0.06	0.10	0.04	0.07	0.01	0.01	0.45	0.48	0.30	0.38	0.11	0.11
HR4362	0.09	0.04	0.05	0.11	0.08	0.01	0.00	0.04	0.06	0.03	0.05	0.01	0.01	0.32	0.35	0.22	0.28	0.13	0.10
SAO050296	0.16	0.04	0.09	0.19	0.06	-0.01	0.01	0.05	0.11	0.03	0.08	0.03	0.02	0.47	0.49	0.32	0.38	0.10	0.09
KYCyg	0.19	0.08	0.08	0.21	0.09	0.03	-0.00	0.09	0.14	0.04	0.10	0.03	0.02	0.51	0.57	0.37	0.46	0.14	0.16
BCCyg	0.18	0.07	0.08	0.18	0.07	0.05	-0.02	0.10	0.11	0.06	0.12	0.02	-0.00	0.43	0.47	0.29	0.39	0.10	0.11
SAO011591	0.17	0.08	0.09	0.17		0.02	0.00	0.08	0.08	0.03	0.07	0.03	0.02	0.47	0.48	0.33	0.38	0.11	0.13
BICyg	0.19	0.08	0.10	0.18	0.08	0.02	-0.02	0.07	0.10	0.02	0.06	0.02	0.02	0.46	0.51	0.34	0.44	0.08	0.11
HR7139	0.08	0.04	0.07	0.15	0.04	0.01	0.01	0.06	0.08	0.05	0.10	0.02	0.01	0.40	0.40	0.25	0.36	0.15	0.12
HR7009	0.06	0.04	0.07	0.16	0.05	0.01	0.01	0.07	0.09	0.04	0.08	0.01	0.01	0.33	0.35	0.22	0.37	0.16	0.12
									GIANTS										
NGC7789k676							0.06	0.04	0.02	-0.01	0.03	0.00	0.02	0.11	0.10	0.06	0.11	0.00	0.04
NGC7789k875							0.04	0.04	0.03	0.04	0.03	0.01	0.02	0.07	0.06	0.04	0.06	0.02	0.03
NGC7789k897							0.01	0.02	-0.02	0.02	-0.03	0.02	0.03	0.06	0.05	0.06	0.06	-0.05	0.04
M67F84	0.10	0.03	0.06	0.06	0.04	0.01	0.01	0.03	0.02	0.01	0.01	0.01	-0.01						
NGC7789k859							0.03	0.03	0.01	0.02	0.01	0.01	0.03	0.10	0.08	0.06	0.09	-0.01	0.04
NGC7789k575							0.03	0.03	0.02	0.01	0.02	0.00	0.02	0.14	0.13	0.09	0.11	0.01	0.04
NGC188I105	0.14	0.05	0.08	0.05	0.08	0.01	0.01	0.04	0.05	0.01	0.02	0.01	0.01	0.19	0.20	0.13	0.14	0.05	0.05
M92XII8	0.03	0.00	0.03	0.01	0.03	0.00	0.03	0.00	-0.01	0.01	-0.00	0.00	0.01	0.01	0.00	0.01	-0.01	-0.00	0.01
NGC188I69	0.16	0.04	0.10	0.07	0.08	0.02	0.00	0.03	0.05	0.02	0.05	0.03	0.03	0.23	0.23	0.15	0.22	0.03	0.07
NGC188II72	0.17	0.03	0.09	0.04	0.06	0.01	0.00	0.03	0.03	0.01	0.03	0.02	0.01	0.22	0.23	0.17	0.16	0.04	0.05
M03IV25	0.02	0.03	0.04	-0.01	0.01	0.01	-0.04	0.01	-0.08	0.00	-0.10	-0.05	-0.08	-0.05	-0.07	-0.07	-0.04	-0.14	0.04
NGC188II181	0.17	0.05	0.10	0.08	0.07	0.02	-0.00	0.04	0.04	0.02	0.04	0.02	0.01	0.23	0.24	0.16	0.19	0.03	0.07
M05IV59						0.00	-0.01	0.01	0.02	0.02	0.03	0.01	-0.00	-0.00	0.03	0.05	0.13	0.03	0.05
NGC7789k468	0.09	0.02	0.09	0.11	0.06	0.01	0.02	0.03	0.02	0.01	-0.00	0.01	0.00	0.21	0.17	0.13	0.19	0.03	0.06
NGC7789k669	0.09	0.02	0.09	0.06	0.04	0.02	0.02	0.03	0.03	0.01	0.01	0.01	0.01	0.20	0.16	0.12	0.20	0.05	0.08
M71A9	0.10	0.03	0.09	0.04	0.07	0.00	0.00	0.01	0.02	0.01	0.03	0.00	0.00	0.21	0.23	0.15	0.20	0.08	0.07
M05IV19						0.01	-0.01	0.03	0.02	0.02	0.02	0.03	0.01	0.01	0.04	0.05	0.14	0.02	0.05

Table 5—*Continued*

Star ID	Mg	Fe	Si	CO	Mg	Mg	Brγ_k	Na	Na	Ca	Ca	Mg	Mg	CO	CO	CO	CO	CO	CO
NGC7789k501	0.10	0.03	0.10	0.09	0.05	0.02	0.02	0.04	0.04	0.02	0.01	0.02	0.02	0.20	0.16	0.12	0.20	0.04	0.07
M71A4	0.11	0.04	0.10	0.07	0.07	0.01	0.00	0.03	0.06	0.01	0.05	0.00	0.02	0.20	0.21	0.13	0.21	0.06	0.06
M71A6	0.11	0.04	0.09	0.09	0.07	0.01	-0.01	0.03	0.05	0.02	0.04	0.01	0.01	0.25	0.27	0.17	0.26	0.15	0.10
M13B786	0.03	0.01	0.04	0.01	-0.01	0.00	0.03	0.01	-0.01	-0.00	-0.02	0.01	0.02	0.04	0.03	0.02	-0.01	-0.00	0.01
NGC7789k971	0.10	0.02	0.09	0.11	0.05	0.02	0.01	0.04	0.02	0.01	0.00	0.01	-0.00	0.29	0.24	0.20	0.26	0.07	0.10
NGC7789k415							0.01	0.04	0.04	0.02	0.03	0.01	0.01	0.27	0.25	0.17	0.24	0.04	0.08
NGC188s359	0.07	0.02	0.06	0.06	0.03	0.01	0.01	0.02	0.02	0.01	0.02	0.01	-0.00	0.23	0.23	0.15	0.20	0.06	0.07
NGC188s473	0.08	0.02	0.07	0.10	0.07	0.01	0.00	0.04	0.05	0.02	0.03	0.02	-0.00	0.26	0.26	0.16	0.22	0.07	0.08
TLE205	0.16	0.05	0.09	0.08	0.07	0.03	-0.01	0.08	0.05	0.03	0.05	0.04	0.04	0.31	0.27	0.17	0.26	0.09	0.10
HR7171	0.04	0.00	0.07	0.00	0.04														
HR5694	0.09	0.03	0.05	0.01	0.04	0.02	0.08	0.01	0.03	0.01	0.02	0.02	0.02	-0.00	0.00	-0.01	0.02	0.00	0.01
HR4883		0.02	0.02	0.02	0.01	0.01	0.06	0.01	0.00	-0.01	-0.00	-0.02	-0.01	0.02	0.02	0.02	0.01	0.01	0.01
HR0163	0.11	0.02	0.08	0.05	0.03														
HR4716	0.06	0.02	0.07	0.02	0.03	0.02	0.05	0.01	0.02	0.01	0.03	0.02	0.02	0.07	0.08	0.04	0.06	-0.00	0.02
HR5480	0.08	0.03	0.10	0.04		0.02	0.04	0.02	0.04	0.02	0.05	0.03	0.03	0.11	0.11	0.05	0.13	0.01	0.04
HR4418	0.07	0.03	0.04	0.04	0.03	0.01	0.04	0.01	0.03	0.01	0.02	0.01	0.02	0.15	0.16	0.12	0.11	0.01	0.04
HR0265	0.12	0.04	0.07	0.03		0.02	0.01	0.03	0.03	0.01	0.03	0.03	0.03	0.15	0.15	0.10	0.16	0.00	0.07
HR5681	0.09	0.03	0.10	0.04	0.04	0.02	0.03	0.02	0.04	0.02	0.03	0.03	0.03	0.11	0.12	0.07	0.13	0.02	0.03
HR5888		0.04	0.06	0.04	0.03	0.02	0.03	0.03	0.03	0.02	0.02	0.01	0.01	0.11	0.12	0.07	0.12	0.01	0.03
HR6770	0.06	0.03	0.04	0.02	0.02	0.01	0.05	0.01	0.02	0.01	0.02	0.01	0.02	0.02	0.03	0.02	0.09	0.01	0.04
HR4932	0.09	0.03	0.07	0.03	0.04	0.02	0.03	0.02	0.03	0.01	0.02	0.03	0.03	0.07	0.07	0.03	0.07	0.01	0.03
HR3427	0.11	0.05	0.08	0.04	0.04	-0.01	0.07	0.03	0.05	0.02	0.04	0.02	0.03	0.12	0.14	0.08	0.12	0.05	0.05
HR4400	0.06	0.02	0.04	0.03	0.02	0.01	0.03	0.01	0.02	0.01	0.02	0.02	0.02	0.09	0.10	0.06	0.10	-0.00	0.04
HR7430	0.13	0.03	0.11	0.04	0.06	0.01	0.02	0.04	0.04	-0.00	0.02	0.02	0.01	0.04	0.05	0.04	0.14	-0.00	0.05
HR2153	0.11	0.02	0.08	0.04	0.04	0.00													
HR5366	0.09	0.03	0.09	0.03	0.04	0.02	0.05	0.02	0.03	0.02	0.03	0.01	0.02	0.14	0.14	0.09	0.13	0.01	0.04
HR2970	0.10	0.03	0.08	0.03	0.07	0.02	-0.00	0.02	0.02	0.02	0.03	0.03	0.03	0.13	0.15	0.09	0.15	0.05	0.09
HR3369										0.01	0.03	0.02	0.02	0.13	0.14	0.08	0.10	0.02	0.03
HR3428	0.10	0.04	0.08	0.07	0.04	0.01	0.03	0.04	0.04	0.02	0.03	0.03	0.01	0.13	0.14	0.09	0.10	-0.00	0.03
SAO121191	0.09	0.03	0.06	0.05	0.04	0.01	0.01	0.05	0.05	0.02	0.03	0.01	0.02	0.13	0.14	0.08	0.16	0.02	0.05
SAO123779	0.07	0.03	0.06	0.04	0.04	0.01	-0.01	-0.00	0.02	-0.00	0.02	0.01	0.00	0.03	0.04	0.05	0.13	-0.00	0.05
SAO082685						0.03													
HR1907										0.02	0.02	0.03	0.03	0.16	0.17	0.11	0.11	-0.00	0.03
HR2701	0.10	0.02	0.08	0.03	0.03	0.02	0.06	0.02	0.02	0.01	0.03	0.02	0.03	0.11	0.12	0.06	0.10	0.02	0.03
HR4287	0.11	0.03	0.08	0.04						0.02	0.05	0.01	0.02	0.17	0.18	0.12	0.18	0.02	0.05
HR3461	0.08	0.04	0.07	0.06	0.02	0.00	0.03	0.01	0.03	0.02	0.01	0.02	0.03	0.19	0.20	0.15	0.16	0.00	0.04
HR3994	0.14	0.03	0.12	0.06	0.06	0.03	0.03	0.02	0.03	0.01	0.02	0.03	0.01	0.11	0.12	0.08	0.12	-0.01	0.06
HR4668	0.08	0.02	0.05	0.05	0.04	0.01	0.01	0.02	0.03	0.01	0.02	0.01	0.01	0.17	0.18	0.12	0.15	0.03	0.05
HR5196	0.06	0.01	0.10	0.04	0.06	0.02	0.04	0.02	0.03	0.01	0.02	0.03	0.03	0.05	0.07	0.06	0.08	0.01	0.04
HR8165	0.10	0.03	0.08	0.05	0.05	0.01	0.01	0.03	0.03	0.02	0.04	0.02	0.02	0.07	0.08	0.06	0.16	0.04	0.05
HR6018	0.11	0.02	0.08	0.04	0.04	0.00	0.07	0.02	0.03	0.02	0.04	0.02	0.02	0.10	0.11	0.05	0.11	0.02	0.04
HR6817	0.10	0.04	0.08	0.03	0.04	0.02	0.02	0.01	0.02	0.01	0.02	0.01	0.01	0.03	0.03	0.03	0.07	0.01	0.02
HR8841	0.08	0.02	0.06	0.04	0.03	0.02	0.03	0.01	0.03	0.01	0.03	0.02	0.02	0.17	0.18	0.13	0.15	0.03	0.05
HR7148	0.14	0.06	0.09	0.05	0.06														
HR7176	0.12	0.03	0.08	0.04	0.04	0.02	0.08	0.02	0.01	0.02	0.02	0.01	0.01	0.03	0.05	0.05	0.13	0.00	0.04
SAO116988	0.08	0.03	0.04	0.01	0.06	0.01	-0.00	0.02	0.03	0.00	0.02	0.01	0.01	0.15	0.17	0.08	0.21	0.00	0.08
HR1779	0.13	0.06	0.10	0.04	0.07	0.01	0.01	0.04	0.05	0.02	0.04	0.02	0.02	0.15	0.15	0.09	0.14	0.01	0.05
SAO060890	0.10	0.04	0.04	0.06	0.02	0.01	0.02	0.03	0.06	0.01	0.04	0.01	0.01	0.19	0.21	0.14	0.16	0.04	0.05
SAO089499	0.08	0.02	0.04	0.01	0.04	-0.00	0.02	0.01	-0.00	0.00	-0.01	0.02	0.02	0.12	0.12	0.11	0.12	-0.01	0.05
HR2600	0.09	0.02	0.06	0.05	0.06	0.03	0.01	0.02	0.03	0.02	0.03	0.00	0.01	0.15	0.17	0.08	0.18	0.06	0.05
HR5616	0.08	0.03	0.07	0.06	0.04	0.01	0.01	0.01	0.03	0.02	0.02	0.01	0.01	0.22	0.23	0.16	0.17	0.01	0.06
HR5947	0.10	0.06	0.08	0.05	0.04	0.02	0.02	0.04	0.03	0.02	0.02	0.00	-0.01	0.11	0.12	0.04	0.16	0.02	0.05
HR0617	0.08	0.02	0.05	0.08	0.03	0.02	0.03	0.01	0.02	0.00	0.02	0.00	0.01	0.14	0.15	0.08	0.15	0.03	0.04
HR6872	0.15	0.05	0.09	0.05	0.06	0.00	0.02	0.04	0.05	0.03	0.04	0.02	0.02	0.18	0.18	0.10	0.19	0.02	0.05

Table 5—*Continued*

Star ID	Mg	Fe	Si	CO	Mg	Mg	Br$\gamma_{\rm k}$	Na	Na	Ca	Ca	Mg	Mg	CO	CO	CO	CO	CO	CO
HR5744						0.01	0.02	0.04	0.05	0.03	0.07	0.02	0.02	0.05	0.07	0.07	0.17	0.03	0.06
HR2697	0.13	0.04	0.09	0.06	0.06	0.01	0.01	0.02	0.04	0.03	0.03	0.05	0.04	0.17	0.18	0.10	0.13	-0.00	0.04
HR5854						0.01	0.02												
HR3905	0.10	0.03	0.06	0.05	0.05	0.01	0.03	0.05	0.07	0.01	0.02	0.03	0.03	0.19	0.19	0.11	0.17	0.03	0.05
HR1726	0.11	0.03	0.10	0.06	0.06	0.03	0.01	0.03	0.03	0.03	0.04	0.02	0.01	0.20	0.21	0.12	0.19	0.06	0.07
HR3845	0.12	0.03	0.09	0.06	0.06	0.02	0.00	0.03	0.05	0.03	0.04	0.01	0.02	0.22	0.25	0.18	0.21	0.04	0.06
HR4521	0.17	0.04	0.11	0.08	0.07	0.02	0.01	0.05	0.06	0.03	0.05	0.02	0.02	0.21	0.19	0.09	0.20	0.04	0.06
HR5582	0.18	0.04	0.12	0.08		0.03	0.00	0.05	0.07	0.03	0.06	0.03	0.03	0.19	0.20	0.10	0.20	0.04	0.04
HR2854	0.12	0.02	0.08	0.08	0.07	0.01	0.02	0.01	0.05	0.02	0.04	0.02	0.02	0.18	0.21	0.13	0.22	0.07	0.06
HR6364	0.08	0.02	0.07	0.07	0.04	0.02	0.02	0.03	0.03	0.02	0.04	0.02	0.02	0.21	0.18	0.11	0.18	0.03	0.06
HR4365	0.11	0.05	0.08	0.06	0.05														
HR1015		0.05	0.09	0.06	0.07	0.02	-0.01	0.02	0.04	0.03	0.04	0.02	0.02	0.17	0.19	0.14	0.17	0.04	0.07
HR7429	0.15	0.06	0.07	0.08	0.06	0.02	0.01	0.03	0.04	0.02	0.05	0.02	0.03	0.20	0.21	0.13	0.19	0.02	0.06
HR7759	0.10	0.04	0.06	0.11	0.04	0.01	0.03	0.06	0.08	0.03	0.06	0.01	0.01	0.09	0.14	0.15	0.30	0.09	0.10
HR5370	0.15	0.05	0.10	0.06	0.07	0.03	-0.01	0.05	0.05	0.03	0.05	0.02	0.03	0.21	0.18	0.12	0.20	0.04	0.07
HR7576	0.17	0.04	0.10	0.07	0.07	0.01	0.01	0.03	0.04	0.03	0.05	0.03	0.02	0.22	0.23	0.14	0.23	0.05	0.06
HR8924	0.17	0.05	0.12	0.06	0.08	0.03	0.01	0.05	0.07	0.03	0.05	0.03	0.03	0.08	0.09	0.05	0.14	0.03	0.05
HR1805	0.13	0.02	0.12	0.10	0.07	0.00	0.00	0.04	0.06	0.03	0.05	0.02	0.02	0.25	0.27	0.17	0.24	0.10	0.09
HR7317	0.12	0.02	0.10	0.09	0.09	0.02	0.00	0.03	0.04	0.02	0.04	0.02	0.02	0.08	0.11	0.11	0.21	0.07	0.07
HD077729	0.14	0.02	0.09	0.08	0.10	0.03	-0.00	0.04	0.05	0.03	0.04	0.03	0.04	0.20	0.24	0.14	0.23	0.11	0.09
HR2574						0.02	0.01	0.00	0.02	0.04	0.06	0.01	0.01	0.20	0.24	0.16	0.19	0.09	0.08
SAO116569	0.03	0.03	0.03	0.05	0.08	0.01	-0.01	0.02	0.02	0.03	-0.02	0.00	-0.01	0.20	0.23	0.13	0.24	-0.00	0.09
HR5600	0.10	0.04	0.06	0.08	0.06	0.03	0.02	0.03	0.05	0.02	0.05	0.02	0.02	0.27	0.29	0.20	0.22	0.03	0.07
HR2503	0.12	0.04	0.07	0.06	0.06	0.02	0.03	0.03	0.05	0.02	0.05	0.02	0.03	0.20	0.22	0.13	0.23	0.06	0.06
HR6136	0.11	0.03	0.08	0.10	0.05														
SAO109474	0.08	0.01	0.06	0.06	0.07	0.00	0.05	0.07	0.06	0.02	-0.00	0.01	0.02	0.25	0.26	0.18	0.24	0.02	0.06
HR4954	0.09	0.09	0.09	0.10	0.05	0.01	0.05	0.01	0.02	0.01	0.03	0.02	0.02	0.29	0.30	0.18	0.22	0.05	0.06
HD139669	0.14	0.05	0.12	0.13	0.06	0.01	0.01	0.06	0.07	0.02	0.04	-0.00	0.02	0.22	0.19	0.14	0.21	0.03	0.06
HR2459	0.15	0.04	0.09	0.12	0.06	0.01	-0.00	0.06	0.07	0.03	0.05	0.03	0.02	0.26	0.27	0.16	0.22	0.07	0.09
HR5690	0.13	0.05	0.10	0.09	0.07	0.02	-0.00	0.03	0.05	0.03	0.05	0.02	0.01	0.29	0.31	0.22	0.24	0.08	0.07
HR0843	0.13	0.05	0.09	0.07	0.08	0.02	-0.00	0.04	0.06	0.03	0.05	0.02	0.02	0.21	0.24	0.16	0.20	0.08	0.08
HR4986	0.10	0.01	0.08	0.10	0.09	0.01	-0.03	0.04	-0.01	0.02	-0.07	-0.01	-0.08	0.07	0.08	0.09	0.14	-0.01	0.12
HR4299	0.10	0.04	0.05	0.12	0.03	0.03	0.01	0.03	0.07	0.02	0.05	0.02	0.01	0.30	0.31	0.19	0.28	0.11	0.09
HR4069	0.07	0.04	0.05	0.14	0.01	0.01	0.00	0.03	0.01	0.03	0.03	0.04	0.01	0.34	0.39	0.30	0.21	0.06	0.08
HR8795	0.12	0.02	0.06	0.10	0.05	-0.00	0.01	0.05	0.06	0.02	0.04	0.01	-0.00	0.26	0.29	0.18	0.25	0.07	0.09
HR5739	0.13	0.02	0.11	0.13	0.09	0.02	0.00	0.07	0.08	0.05	0.06	0.03	0.03	0.21	0.24	0.18	0.27	0.10	0.10
HR5800	0.05	-0.00	0.02	0.02	0.05	0.05	0.01	0.01	0.02	0.03	0.03	0.01	-0.01	0.27	0.30	0.20	0.23	0.10	0.07
HR8860	0.10	0.02	0.06	0.13	0.09	0.01	0.00	0.03	0.07	0.02	0.05	0.01	0.01	0.35	0.38	0.24	0.28	0.06	0.07
HR5932	0.07	0.03	0.06	0.10	0.07	0.01	0.03	0.06	0.07	0.02	0.04	0.00	0.00	0.35	0.38	0.27	0.26	0.12	0.09
HR6815	0.14	0.05	0.09	0.14	0.09	0.02	-0.00	0.06	0.07	0.04	0.05	0.02	0.02	0.30	0.33	0.22	0.29	0.09	0.10
HR4184	0.08	0.08	0.08	0.14	0.11	0.01	0.01	0.03	0.05	0.02	0.01	0.02	0.00	0.38	0.45	0.31	0.29	0.09	0.11
B133	0.12	0.03	0.07	0.09	0.05	0.02	0.01	0.06	0.05	0.02	0.08	0.04	0.04	0.32	0.36	0.23	0.26	0.07	0.08
HR6242	0.08	0.05	0.06	0.15	0.07	0.01	0.01	0.06	0.07	0.05	0.09	0.02	-0.00	0.32	0.35	0.22	0.29	0.10	0.08
SAO050381	0.13	0.04	0.11	0.16	0.07	-0.01	0.01	0.06	0.09	0.03	0.06	0.02	0.00	0.36	0.39	0.22	0.30	0.11	0.09
SAO044383	0.09	0.03	0.05	0.15	0.11	0.01	-0.01	0.05	0.04	0.04	0.03	0.03	-0.00	0.38	0.39	0.30	0.27	0.17	0.12
HR4267						0.02	0.01	0.07	0.10	0.04	0.08	0.01	0.02	0.35	0.37	0.25	0.30	0.16	0.11
HR0867	0.07	0.03	0.02	0.16	0.09	0.00	0.01	0.06	0.09	0.04	0.06	0.01	0.01	0.31	0.35	0.25	0.25	0.08	0.08
HR6146	0.08	0.03	0.05	0.16	0.08	0.01	0.00	0.07	0.09	0.04	0.07	0.01	-0.00	0.44	0.50	0.34	0.37	0.10	0.09
BMB194	0.13	0.04	0.08	0.17	0.10	0.04	-0.05	0.05	-0.02	-0.03	-0.09	0.05	0.03	0.24	0.20	0.19	0.15	0.08	0.10
BMB239	0.12	0.04	0.07	0.14	0.05	0.02	-0.01	0.09	0.09	0.05	0.06	0.02	-0.01	0.38	0.34	0.20	0.29	0.12	0.12
BMB179	0.10	0.05	0.06	0.13	0.07	0.02	0.01	0.10	0.10	0.05	0.13	0.04	0.04	0.44	0.45	0.28	0.33	0.06	0.08
BMB181	0.14	0.06	0.08	0.15	0.12	0.03	0.00	0.07	0.10	0.03	0.08	0.03	0.00	0.43	0.42	0.26	0.35	0.14	0.13
BMB285	0.13	0.00	0.02	0.05	0.02	0.02	0.02	0.02	0.04	0.02	0.10	0.07	0.11	0.41	0.44	0.26	0.26	0.05	0.07
BMB087				-0.03	-0.01	0.02	0.03	-0.02	0.03	0.03	0.05	0.02	-0.01	0.17	0.16	0.10	0.12	0.03	0.09

Table 5—*Continued*

Star ID	Mg	Fe	Si	CO	Mg	Mg	Brγ_k	Na	Na	Ca	Ca	Mg	Mg	CO	CO	CO	CO	CO	CO
BMB142	0.09	-0.02	0.06	0.12	0.07	0.02	0.02	0.09	0.11	0.05	0.15	0.04	0.04	0.43	0.47	0.29	0.40	0.10	0.10
BMB039	0.13	0.03	0.07	0.09	0.06	0.05	0.05	0.03	0.08	-0.00	0.06	0.05	0.06	0.35	0.35	0.21	0.23	0.12	0.11
BMB289	0.11	0.03	0.11	0.16	0.07	0.02	-0.02	0.06	0.06	0.03	0.07	0.03	0.01	0.42	0.38	0.24	0.32	0.11	0.11
								DWARFS											
HR3314	0.00	-0.02	0.03	-0.04	0.00	0.00	0.17	0.00	0.01	0.00	0.00	0.00	0.00	0.01	0.01	0.01	-0.00	0.02	0.01
HR5144	0.02	-0.00	0.05	0.01	0.01														
HR3481	0.01	-0.03	0.05	-0.00	-0.01	-0.00	0.15	-0.02	0.03	0.03	0.04	0.00	0.00						
HR4380	0.00	-0.02	0.04	-0.02	-0.00	0.00	0.22	0.00	-0.01	0.00	-0.00	0.01	0.01	-0.00	-0.00	-0.01	-0.01	-0.00	0.01
HR7451	0.04	0.01	-0.00	-0.00	0.01														
HR5270	0.00	-0.01	0.03	-0.00	-0.00	-0.00	0.02	0.01	0.00	-0.00	-0.01	-0.00	-0.01	0.00	0.01	0.01	-0.00	0.00	0.00
HR4785							-0.01	-0.02	-0.01	0.03	0.04	0.02	0.01	0.01	0.01	0.01	0.03	0.02	0.02
HR6212	0.06	0.01	0.07	0.01	0.03	0.01	0.05	0.02	0.02	0.02	0.03	0.02	0.01	0.02	0.01	0.01	0.02	-0.01	0.01
HR5235		0.01	0.06	0.02	0.03	0.00	0.08	0.02	0.02	0.02	0.02	0.02	0.01	0.01	0.01	0.00	0.01	-0.01	0.01
HR5829	0.13	0.03	0.09	0.09	0.07	0.03	-0.00	0.03	0.05	0.01	0.04	0.02	0.03	0.28	0.24	0.15	0.23	0.09	0.05
HR5409	0.06	0.01	0.05	0.01	0.02	0.03	0.05	0.02	0.02	0.01	0.01	0.01	0.02	0.02	0.02	0.00	0.02	0.00	0.02
HR3538	0.10	0.03	0.08			0.02	-0.02	0.04	0.02	-0.01	-0.03	0.01	0.02	-0.02	-0.02	-0.04	0.01	-0.04	0.02
HR5853	0.09	0.02	0.06	-0.00	0.04	0.01	0.07	0.02	0.02	0.01	0.02	0.01	0.01	0.01	0.00	-0.01	0.01	0.01	0.01
HR5072	0.08	0.01	0.05	-0.01	0.03	0.02	0.10	0.00	0.01	0.00	0.00	0.02	0.02	0.02	0.02	0.01	0.03	-0.00	0.01
HR6623	0.09	0.02	0.09	0.05	0.04	0.02	0.04	0.02	0.01	0.01	0.00	0.03	0.02	0.04	0.04	0.02	0.03	-0.02	0.03
HR5019	0.18	0.05	0.08	0.04	0.08	0.02	0.00	0.03	0.03	0.02	0.03	0.02	0.03	0.05	0.04	0.01	0.05	0.01	0.02
HR3259	0.13	0.04	0.06	0.00	0.09	0.00	0.03	0.01	0.03	0.01	0.01	0.00	0.02	0.01	0.02	0.04	0.01	0.07	0.02
SAO074439	0.07	0.01	0.07	0.06	0.03	0.01	0.06	0.01	-0.02	-0.00	-0.05	0.01	-0.02	0.02	0.03	0.03	-0.03	-0.06	0.02
HR4496	0.11	0.02	0.06	0.02	0.05	0.02	0.03	0.02	0.02	0.02	0.03	0.02	0.01	0.02	0.03	0.01	0.02	0.00	0.01
SAO011620	0.14	0.05	0.06	0.04		0.02	0.00	0.03	0.04	0.02	0.03	0.03	0.03	0.13	0.14	0.09	0.14	0.02	0.05
HR7957	0.05	0.01	0.06	0.01	0.02	0.02	0.05	0.01	0.01	0.01	0.01	0.01	0.01	0.08	0.07	0.03	0.10	-0.03	0.04
HR6752	0.16	0.02	0.07	0.02	0.07	0.02	0.23	0.00	0.01	0.01	0.03	0.02	0.03	0.11	0.12	0.08	0.09	-0.00	0.09
SAO074175	0.17	0.04	0.06	0.01	0.07	0.02	0.06	0.00	0.05	0.01	0.02	0.03	0.03	0.06	0.06	0.04	0.13	0.01	0.06
SAO045933	0.15	0.05	0.07	0.02	0.08	0.03	0.02	0.03	0.04	0.01	0.02	0.04	0.03	0.06	0.06	0.02	0.07	-0.00	0.04
HR1325	0.08	0.03	0.01	0.00	0.06	0.00	0.01	0.03	0.04	0.02	0.04	0.03	0.02	0.07	0.08	0.04	0.09	0.07	0.04
HR5553	0.14	0.03	0.07	0.03	0.07	0.03	0.05	0.04	0.05	0.02	0.05	0.03	0.03	0.07	0.07	0.03	0.05	0.00	0.02
HR5901	0.10	0.02	0.05	0.01	0.03	0.05	0.01	0.02	0.02	0.02	0.00	0.02	-0.00	0.07	0.09	0.05	0.06	-0.03	0.04
SAO074883	0.13	0.03	0.04	0.01	0.07	0.02	0.02	0.01	0.03	0.00	0.02	0.02	0.04	0.00	0.00	-0.01	0.03	-0.01	0.03
SAO050265	0.13	0.02	0.12	0.03	0.04	0.01	0.02	0.02	0.02	0.01	0.03	0.02	0.02	0.10	0.10	0.06	0.09	-0.01	0.04
HR6014	0.10	0.02	0.07	0.03	0.05	0.01	0.06	0.03	0.03	0.01	0.03	0.02	0.02	0.11	0.11	0.06	0.15	0.00	0.04
SAO109471	0.14	0.02	0.06	0.00	0.07	0.02	-0.00	0.04	0.04	0.01	0.03	0.02	0.03	0.07	0.08	0.05	0.05	0.01	0.02
SAO028414							0.01	0.03	0.02	0.02	0.03	0.02	0.02	0.04	0.03	0.04	0.06	0.03	0.04
SAO031745	0.12	0.02	0.06	0.01	0.07														
SAO122610	0.13	0.02	0.05	0.02	0.09	0.03	-0.02	0.04	0.05	0.02	0.04	0.03	0.02	0.05	0.04	0.04	0.09	-0.01	0.04
HR8832	0.23	0.03	0.08	0.07	0.12	0.01	-0.01	0.05	0.06	0.03	0.04	0.03	0.03	0.11	0.11	0.07	0.11	0.00	0.04
GJ570A	0.30	0.08	0.09	0.06	0.14	0.06	-0.03	0.07	0.09	0.03	0.06	0.03	0.04	0.11	0.12	0.06	0.08	-0.03	0.04
HR8085	0.15	0.03	0.05	0.00	0.10	0.02	0.03	0.03	0.04	0.04	0.05	0.03	0.03	0.10	0.09	0.04	0.08	-0.00	0.04
GJ380	0.20	0.04	0.07	0.04	0.15	0.03	0.01	0.07	0.11	0.05	0.09	0.04	0.04	0.07	0.08	0.02	0.12	-0.02	0.04
HR8086	0.13	0.03	0.04	0.03	0.11	0.03	0.04	0.07	0.08	0.04	0.05	0.03	0.01	0.12	0.11	0.07	0.09	-0.00	0.04
GJ673	0.17	0.04	0.07	0.03	0.13		-0.02	0.06	0.07	0.08	0.09	0.04	0.04	0.07	0.06	0.04	0.06	-0.02	0.03
SAO027179	0.17	0.03	0.05	0.02	0.12	0.02	0.02	0.09	0.12	0.04	0.07	0.01	0.01	0.10	0.10	0.08	0.06	0.01	0.02
GJ625								0.07	0.05	0.03	0.02	0.01	0.02	0.04	0.03	0.03	0.02	-0.02	0.01
GJ570B	0.20	0.05	0.04	0.02	0.13	0.03	-0.01	0.11	0.14	0.07	0.08	0.02	0.02	0.13	0.14	0.09	0.08	-0.03	0.05
GJ015SW	0.09	0.01	-0.01	-0.01	0.07	0.01	0.08	0.09	0.09	0.05	0.07	0.01	0.02	0.13	0.14	0.12	0.08	-0.00	0.02
GJ411	0.05	0.01	0.02	0.01	0.11	0.02	0.01	0.02	0.04	0.01	0.02	-0.01	-0.02	0.08	0.07	0.04	0.02		0.01
GJ412A						0.02	-0.00	0.05	0.07	0.02	0.07	0.01	0.01	0.06	0.07	0.04	0.08		0.03
GJ526	0.10	0.01	0.02	0.01	0.10	0.01	0.01	0.05	0.08	0.02	0.06	0.01	-0.00	0.09	0.10	0.06	0.08	0.01	0.02
GJ388	0.09	0.00	0.02	0.04	0.07	0.01	0.01	0.09	0.12	0.07	0.11	0.00	-0.00	0.11	0.11	0.08	0.11	0.00	0.04
GJ725A	0.06	0.00	0.00	0.00	0.08		0.15	0.05	0.04	0.05	0.02	0.02	0.00	0.03	0.02	0.01	-0.00	-0.02	0.02

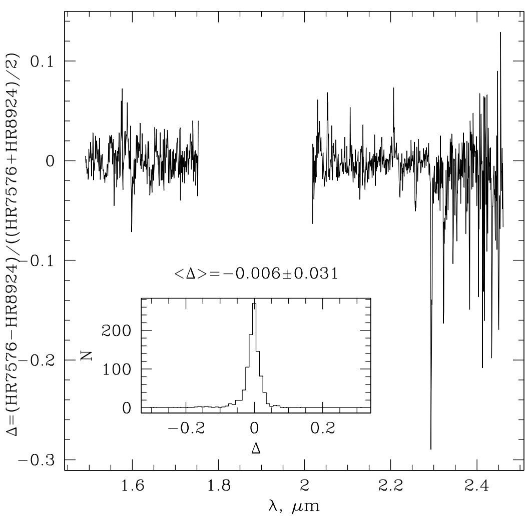

Fig. 1.— Data quality: difference Δ between the spectra of two K3 III stars – HR 7576 and HR 8924 – with similar abundances, normalized by the average of the two spectra as a function of wavelength (in arbitrary flux units). The inset shows the histogram of the differences. The means and the standard deviation of the distribution are also shown.

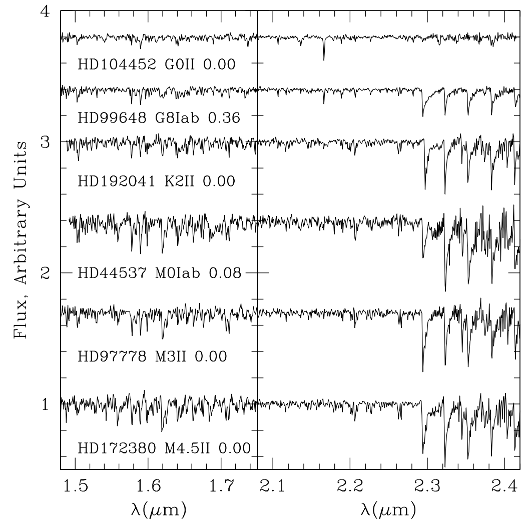

Fig. 2.— A subset of H and K spectra of supergiants. The names of the stars, spectral types, and [Fe/H] are indicated. The spectra are continuum divided and shifted vertically for display purposes by adding (from bottom to top): 0.0, 0.7, 1.4, 2.0, 2.4, and 2.8.

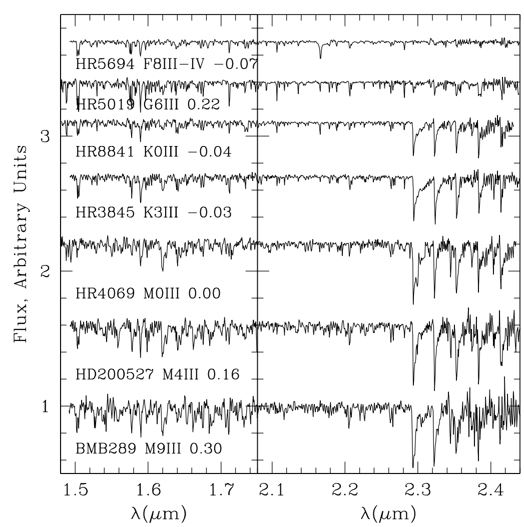

Fig. 3.— A subset of H and K spectra of giants. The names of the stars, spectral types, and [Fe/H] are indicated. The spectra are continuum divided and shifted vertically for display purposes by adding (from bottom to top): 0.0, 0.6, 1.2, 1.7, 2.1, 2.4, and 2.7.

Table 5—*Continued*

Star ID	Mg	Fe	Si	CO	Mg	Mg	Brγ_k	Na	Na	Ca	Ca	Mg	Mg	CO	CO	CO	CO	CO	CO
GJ015NE	0.02	-0.03	-0.02	-0.01	0.01	-0.00	0.00	0.08	0.06	-0.00	0.02	-0.00	0.01	0.12	0.12	0.09	0.05	0.01	0.02
GJ402	0.02	0.01	-0.02	0.01	0.04	-0.00	-0.02	0.13	0.13	0.03	0.04	0.00	-0.01	0.09	0.09	0.07	0.07	-0.02	0.04
GJ213	0.00	-0.01	-0.03	-0.01	0.02	-0.00	0.03	0.08	0.08	0.04	0.07	0.00	0.00	0.10	0.11	0.06	0.06	0.00	0.03
GJ206	0.03	0.01	-0.02	0.01	0.05	-0.01	0.01	0.06	0.08	0.06	0.08	0.01	0.00	0.12	0.12	0.07	0.07	0.02	0.03
GJ831	-0.01	-0.02	-0.03	-0.01	0.03	-0.00	-0.01	0.06	0.08	0.02	0.06	0.00	0.02	0.07	0.09	0.06	0.12	-0.01	0.05
GJ866A	0.00	-0.03	-0.01	-0.04	-0.01	-0.00	-0.01	0.10	0.12	-0.01	0.00	-0.00	-0.02	0.15	0.16	0.11	0.08	-0.03	0.04
GJ065	-0.01	-0.00	-0.01	-0.04	-0.01	0.01	0.04	0.07	0.09	0.01	0.03	0.01	0.02	0.12	0.13	0.08	0.10	0.00	0.02
GJ905	0.01					-0.00	0.02	0.15	0.14	0.00	0.03	-0.00	0.00	0.14	0.14	0.12	0.13	0.00	0.04

Note.—Indices are given in magnitudes. The numbers in the heading correspond to the numbers of index definitions given in Table 4. Stars are sorted in order of luminosity and spectral class, same as in Table 3. The complete table is presented in the electronic edition.

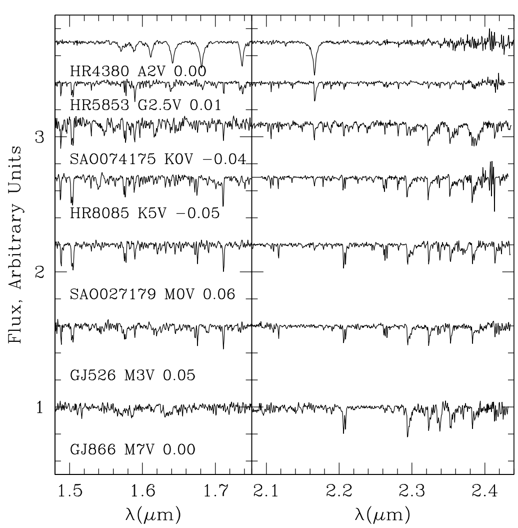

Fig. 4.— A subset of H and K spectra of main sequence stars. The names of the stars, spectral types, and [Fe/H] are indicated. The spectra are continuum divided and shifted vertically for display purposes by adding (from bottom to top): 0.0, 0.6, 1.2, 1.7, 2.1, 2.4, and 2.7.

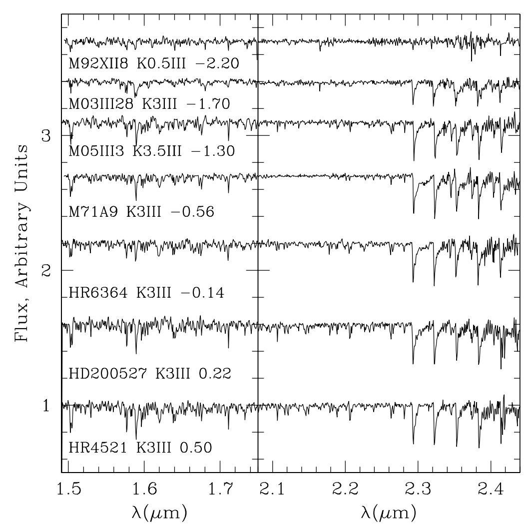

Fig. 5.— A subset of H and K spectra for a selection of K giants spanning a range of metallicities. The names of the stars, spectral types, and [Fe/H] are indicated. The spectra are continuum divided and shifted vertically for display purposes by adding (from bottom to top): 0.0, 0.6, 1.2, 1.7, 2.1, 2.4, and 2.7.

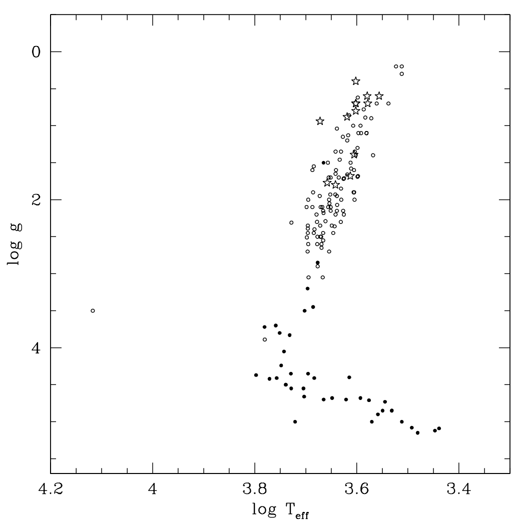

Fig. 6.— Content of the library: distribution of the library stars on the surface gravity $\log g$ versus effective temperature $T_{\rm eff}$ plane. Star symbols are supergiants, circles are giants, and solid dots are sub-giants and dwarfs. The "anomalous" subgiant at $\log g$=1.5 is extremely metal poor, with [Fe/H]=−2.67.

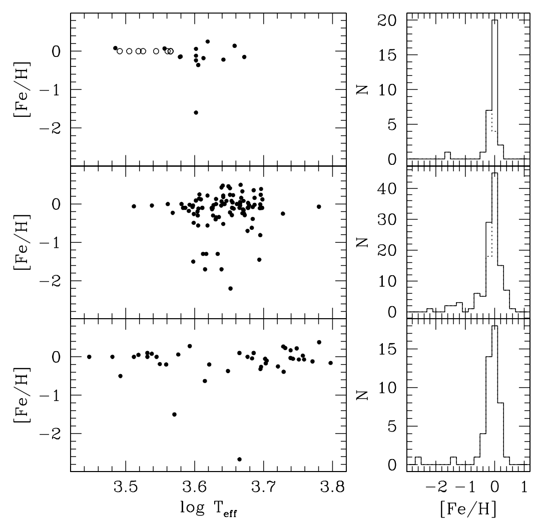

Fig. 7.— Metallicity of library stars [Fe/H] versus the effective temperature $T_{\rm eff}$ (left panels), and metallicity histograms (right) for supergiants, giants, and dwarfs (from top to bottom). The stars with parameters adopted from the literature are shown with solid dots, and the stars with asummed parameters are circles. Solid-line histograms include all stars with adopted or asummed metallicity, and dotted-line histograms omit the asummed values.

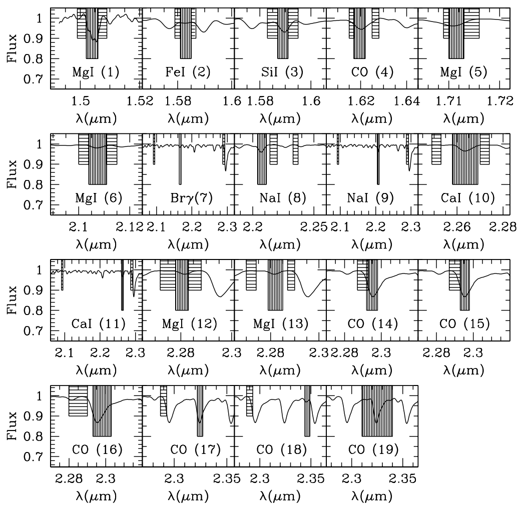

Fig. 8.— Definitions of the spectral indices. The vertically shaded area represents the line band, and the horizontally shaded areas are the continuum bands. Note that the last index is measured after the continuum normalization over the entire K spectra, and has no proper continuum band. The bracketed numbers in each panel correspond to the index numbering in Table 4.

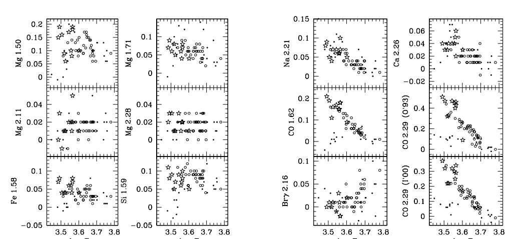

Fig. 9.— Line indices as temperature indicators. The Si and the CO (upper panel) definitions are from Origlia, Moorwood & Oliva (1993), the Brγ is from Kleinmann & Hall (1986), the CO (lower panel) is from Ivanov et al. (2000), and all MgI and Fe indices are from this work. Star symbols indicate supergiants, open circles are giants, and solid dots represent dwarfs and sub-giants. All indices are in magnitudes. The typical measurement error is σ=0.02 mag. Only stars with $-0.10 \leq$[Fe/H]$\leq +0.10$ are shown.

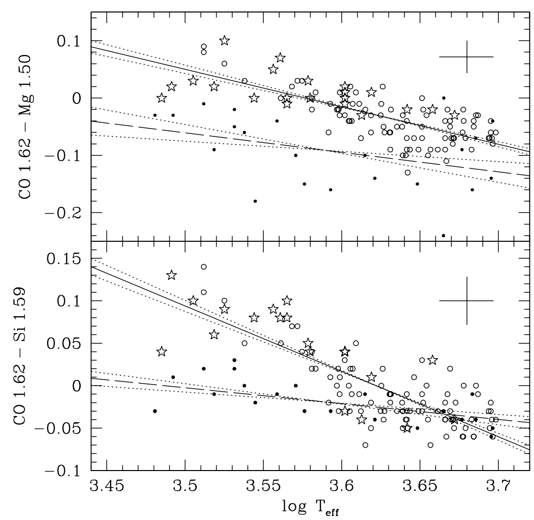

Fig. 10.— Line ratios as temperature indicators. The CO and SiI definitions are from Origlia, Moorwood & Oliva (1993), and the MgI is from this work. All indices are in magnitudes. Star symbols indicate supergiants, open circles are giants, and solid dots represent dwarfs and sub-giants. The typical $\pm 1\sigma$ measurement error is shown in the top right corner. The best linear fits to supergiants and giant are shown with a solid line, and the best fit to dwarfs and subgiants is a dashed line. The dotted lines represent $\pm 1\sigma$ errors in the slopes.

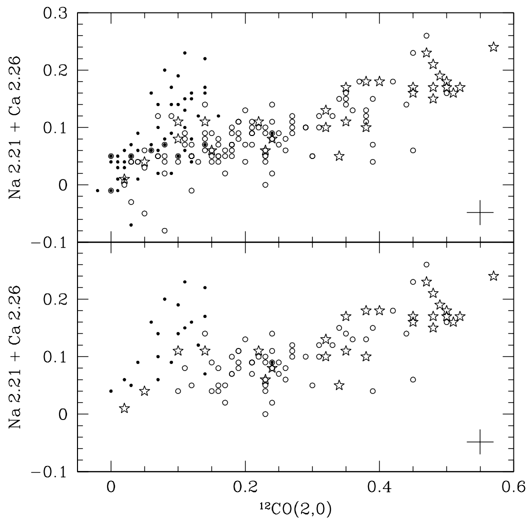

Fig. 11.— Two-dimensional Spectral Classification. Comparison of the strengths of Na and Ca features, with the 2.29μm CO bandhead absorption, following Kleinmann & Hall (1986). All index definitions are from there and the indices are in magnitudes. Star symbols indicate supergiants, open circles are giants, and solid dots represent dwarfs and sub-giants. The typical $\pm 1\sigma$ observational uncertainties are shown in the bottom right corner. The top panel includes all stars, the bottom panel shows only stars with [Fe/H]≥ -0.5 and $T_{\rm eff} \leq 4500$ K.

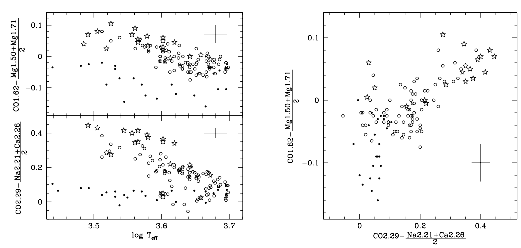

Fig. 12.— Two-dimensional Spectral Classification with H-band features (top) and K-band features (bottom). All indices are in magnitudes. The stellar effective temperature $T_{\rm eff}$ is used on the left plot, and only pure observables are used on the right. Star symbols indicate supergiants, open circles are giants, and solid dots represent dwarfs and sub-giants. The typical $\pm 1\sigma$ measurement error is shown in the bottom right corner. The CO bands are defined by Origlia, Moorwood & Oliva (1993), the Ca and Na indices are from Ali et al. (1995), and the Mg definitions are from this work.